ALKOR-Berichte

# *Dynamics and variability of POC burial in depocenters of the North Sea (Skagerrak)*

Cruise No. AL561

2.08.2021 – 13.08.2021

Kiel – Kiel

APOC

Mark Schmidt, Stefan Sommer, Christoph Böttner, Andrew Dale, Nina Lenz, Timo Spiegel

Chief Scientist Mark Schmidt

GEOMAR Helmholtz Centre for Ocean Research Kiel

2021

## Table of Contents

# 1 Cruise Summary

## 1.1 Summary in English

The AL561 cruise was conducted in the framework of the project APOC ("**A**nthropogenic impacts on **P**articulate **O**rganic **C**arbon cycling in the North Sea"). This collaborative project between GEOMAR, AWI, HEREON, UHH, and BUND is to understand how particulate organic carbon (POC) cycling contributes to carbon sequestration in the North Sea and how this ecosystem service is compromised and interlinked with global change and a range of human pressures include fisheries (pelagic fisheries, bottom trawling), resource extraction (sand mining), sediment management (dredging and disposal of dredged sediments) and eutrophication. The main aim of the sampling activity during AL561 cruise was to recover undisturbed sediment from high accumulation sites in the Skagerrak/Kattegat and to subsample sediment/porewater at high resolution in order to investigate sedimentation transport processes, origin of sediment/POC and mineralization processes over the last 100- 200 years. Moreover, the actual processes of sedimentation and POC degradation in the water column and benthic layer will be addressed by sampling with CTD and Lander devices. In total 9 hydroacoustic surveys (59 profiles), 4 Gravity Corer, 7 Multicorer, 3 Lander and 4 CTD stations were successfully conducted during the AL561 cruise.

## 1.2 Zusammenfassung

Die hier beantragte Forschungsfahrt wurde im Rahmen eines vom BMBF finanzierten Verbundprojektes "APOC" durchgeführt. Die Verbundpartner GEOMAR, AWI, HEREON, UHH, BUND im Projekt APOC wollen klären, wie der Eintrag, Transport und Abbau von partikulären organischen Kohlenstoffs (POC) zur Fixierung von Kohlenstoff in den Nordseesedimenten beiträgt und wie diese Ökosystemleistung durch den globalen Wandel und anthropogenen Nutzungsdruck (Fischerei, Rohstoffgewinnung, Sedimentmanagement, Eutrophierung) beeinträchtigt wird. Da ein wesentlicher Anteil der aus der Nordsee stammenden re-suspendierten POC/Feinfracht im Skagerrak und dem Norwegischen Graben abgelagert wird, wurden im Rahmen der AL561-Expedition Sediment-Proben aus dem tiefen Skagerrak geborgen. Hochauflösende Sediment/Porenwasserbeprobungen wurden an Bord durchgeführt, um daran, mithilfe verschiedenster geochemischer Analyse und Modellierungsverfahren, die Sedimentationsbedingungen, die Herkunft der Sedimente und des POC, sowie biogeochemische Prozesse der Mineralisierung von POC untersuchen zu können. Insbesondere soll die zeitliche Variabilität (aktuell – 200 y.b.p.) dieser Charakteristika untersucht werden. Die aktuellen Sedimentationsbedingungen sollen anhand von suspendiertem Material, welches aus der Wassersäule mittels CTD-Beprobung und Filtration gewonnen wurde und anhand von benthischen Kammerproben, welche über Lander Einsätze gewonnenen wurden, genauer untersucht werden. Insgesamt wurden 9 hydroakustische Vermessungen (59 Profile), 4 Schwerelot, 7 Multicorer, 3 Lander und 4 CTD Stationen während der AL561 erfolgreich durchgeführt.

# 2 Participants

## 2.1 Principal Investigators

| Name | Institution |
|---|---|
| Schmidt, Mark, Dr. habil. | GEOMAR |
| Sommer, Stefan, Dr. | GEOMAR |
| Dale, Andrew, Dr. | GEOMAR |
| Böttner, Christoph, Dr. | CAU |

## 2.2 Scientific Party

| Name | Discipline | Institution |
|---|---|---|
| Schmidt, Mark, Dr. habil. | Biogeochemisty / Chief Scientist | GEOMAR |
| Sommer, Stefan, Dr. | Benthic processes / Co-Chief Scientist | GEOMAR |
| Dale, Andrew, Dr. | Porewater Biogeochemistry | GEOMAR |
| Böttner, Christoph, Dr. | Geophysics/Sedimentology | CAU |
| Lenz, Nina, PhD student | Metal tracer, Sedimentology | GEOMAR |
| Spiegel, Timo, PhD student | Porewater Biogeochemistry | GEOMAR |
| Domeyer, Bettina | Lab-Technician | GEOMAR |
| Surberg, Regina | Lab-Technician | GEOMAR |
| Türk, Matthias | BIGO technician | GEOMAR |
| Petersen, Asmus | Coring technician | GEOMAR |

## 2.3 Participating Institutions

GEOMAR Helmholtz Centre for Ocean Research Kiel
CAU Marine Geophysics, Christian-Albrechts-University Kiel

# 3 Research Program

## 3.1 Description of the Work Area

The burial of particulate organic carbon (POC) in the North Sea is focused on depocenters like the deep Skagerrak where fine-grained material (mud) is deposited due to low bottom current velocities (e.g. Rodhe 1996; de Haas et al., 2002; Ståhl et al., 2004; Diesing et al., 2021). The mud accumulating at the seabed is composed of marine POC flocculated with terrigenous fine material. The highest sedimentation rates (11 mm/yr) and POC contents (~3 wt.%) in the North Sea are found in the central part of the Skagerrak (Fig. 3.1; e.g. de Haas and van Weering, 1997). The terrigenous mud and autochtonous marine particles are transported and redistributed by a tidally and wind driven current regime across the North Sea and Baltic shelf, entering the Skagerrak by forming a cyclonic current pattern (Fig. 3.1). The cyclonic current system reaches down to 400-500 m water depths, with a mainly stagnant water mass below (Rodhe et al, 1996).

The origin and transport pathways of the sediment deposited in the Skagerrak are reflected by its mineralogy, trace metal composition and isotope ratios of radiogenic elements of fine-grained sediment fraction. Detrital sediment originating from weathering of Precambrian Scandinavian rocks exhibits low $^{176}Hf/^{177}Hf$- and $^{143}Nd/^{144}Nd$-ratios but high $^{87}Sr/^{86}Sr$-ratios. Whereas terrigenous sediment transported from central European rivers towards the North Sea are mainly characterized by high $^{176}Hf/^{177}Hf$- and $^{143}Nd/^{144}Nd$-ratios and low $^{87}Sr/^{86}Sr$-ratios. The clay mineral composition of the Northern North Sea dominated by illite and chlorite differs from smectite-dominated German Bight (e.g. Irion and Zöllmer, 1999). Moreover, radio-nuclides adsorbed to fine-grained organic-rich sediment serve as markers for time events and their transport pathways, e.g. beside lead the Chernobyl $^{137}Cs$ was predominantly transported from Elbe and Rhine into the Skagerrak depocenter (Kuijpers et al., 1993).

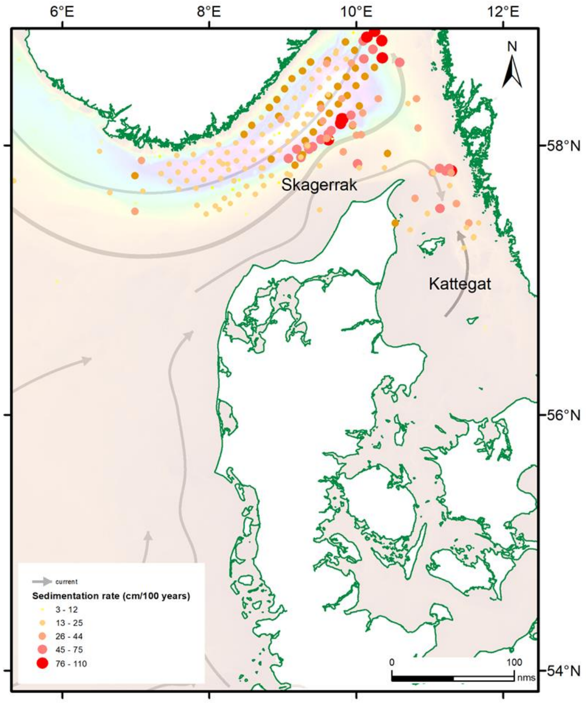


**Fig. 3.1** Sedimentation rates in the area of investigation (de Haas et al., 1997; de Haas et al., 1996; de Haas and van Weering, 1997; European Atlas of the Seas, 2021). Gray arrows depict the major current patterns.

## 3.2 Aims of the Cruise

The AL561 research cruise was focusing on recovering surface sediment (0-3 m bsf) from the Skagerrak/Kattegat by coring and subsampling sediment/porewater at high resolution in order to investigate the origin of sediment/POC, sediment transport processes, and mineralization processes with time (recent – 200 years b.p.). Moreover, the actual processes of sedimentation and respiration in the water column and benthic layer were addressed by sampling with CTD-Rosette and Lander devices.

The mineralogical, (bio)geochemical, and radio-tracer analyses performed on sampled sediment/porewater will help to answer the question on when and how POC burial changed over the last two centuries in the North Sea. The analyzed data will be used in a model, which is based on the Geesthacht Coupled cOAstal model SysTem (GCOAST) to simulate the pelagic and benthic turnover of POC considering biogeochemical processes, food web carbon transfer and the physical dynamics of fine-grained lithogenic particles transported into the North Sea depocenters. In conjunction with current patterns of the North Sea the analytical data constrains the GCOAST model to address how and when human pressures (e.g. offshore construction; trawling; coastal management, etc.) affected turnover and burial of POC in depocenters like the Skagerrak.

### 3.3 Agenda of the Cruise

The agenda of the cruise was to start with hydroacoustic monitoring in the approved sampling areas in the Skagerrak (and Kattegat). Sediment depths morphology and subbottom stratigraphy had to be characterized on multiple tracks in the areas N1-N4 and S1 (Fig. 3.2) with shipborne echosounder EK60 and INNOMAR sub bottom profiler. The hydroacoustic data evaluation had to consider small scale depressions and highs and to indicate sediment erosion features, buried turbidites and shallow gas. The subsurface (Holocene) sediment stratigraphy mainly determined during night was the basis to select coring sites for retrieving undisturbed sediment cores with high temporal resolution of the last two centuries. Preferably multi-coring was considered for coring of up to 0.6 m of undisturbed young sediment and for subsequent high-resolution (1 cm slices) sediment sampling. A gravity corer (<3 m) had to be used for recovering deeper sediment to reconstruct the overall Holocene setting of the sampling site. Porewater, sediment, and headspace gas sampling of MUC and GC had to be conducted to constrain diagenetic transport and degradation processes in the younger surface sediment.
A benthic lander had to be deployed during the research cruise to define benthic fluxes relevant for POC degradation and release of nutrients and C-species at the sediment-water interface. Water column and ambient bottom water samples taken by a Video-CTD Rosette equipped with Niskin water sample bottles and various sensors should give insights into the origin of the actual origin of water masses and suspended particulate matter (SPM). Where high turbidity was indicated by sensor measurements during hydrocasts SPM sampling by onboard vacuum filtration had to be conducted to define e.g. the origin and transport paths of fine-grained particles actually settling in the Skagerrak.

All sediment and (pore)water samples will be analyzed extensively onshore by e.g. high-resolution grain size and structure/geometry analysis (X-ray) onshore to gain interpretational basis on e.g. bioturbation and bottom-current energy of the past. Sediment samples will be age-dated using a range of isotope methods ($^{210}$Pb, $^{137}$Cs, $^{14}$C) to reconstruct changes in mass accumulation rates. Radio isotope activity concentrations will be determined and lead isotope ratios ($^{206/207}$Pb, $^{206/208}$Pb) will be analyzed to characterize anthropogenic gasoline time frame.
Mineral contents, grain size distributions, and trace elements as well as stable isotope ratios and signatures (e.g. $^{87}$Sr/$^{86}$Sr, Nd isotopes, stable Fe isotopes) will be analyzed to decipher the provenance of the terrigenous particles (e.g. North Sea, Baltic Sea, North Atlantic, Scandinavian margin). The data will be evaluated to reconstruct changes in the sediment supply from the North Sea and identify possible anthropogenic effects on sediment delivery and transport. A range of geochemical and biogeochemical parameters will be measured in sediments and filtered particulate matter (TOC, inorganic carbon, total N, total S, chlorophyll-a) and pore fluids

(dissolved ammonium, phosphate, iron, manganese, silica, sulfate, chloride, methane). Subsamples of sediment will be digested (Total alkaline digest) to analyze major and trace element composition by using ICP-OES and ICP-MS. Moreover, radiogenic $^{87}Sr/^{86}Sr$-, $^{176}Hf/^{177}Hf$- and $^{143}Nd/^{144}Nd$ ratios will be determined by using multi-collector-ICP-MS. The origin, reactivity/freshness and age of particulate organic matter will be assessed by both $^{15}N$ and by applying state-of-the-art organic geochemical methods relying on lipid biomarker analysis, and $^{14}C$ analyses of bulk organic carbon and specific compounds using the MICADAS system at AWI. By comparing the $^{14}C$ signatures of sedimentary POC from different sources along transport trajectories, time-scales of degradation and POC stabilization mechanisms can be determined. Routine XRD measurement at GEOMAR will be used to identify general mineral composition of sediment. Grain size distribution and BET mineral surface will be determined.

1D inverse transport-reaction modelling will be conducted at GEOMAR after the cruise with sediment/porewater chemistry and precise age dating results to reconstruct historical POC variations at the seafloor (z=0 cm) in the Skagerrak. The modelled POC data will then be used by the APOC consortium to constrain lateral POC transport under changing environmental conditions in the North Sea, by applying different scenarios of natural (climatic) changes and anthropogenic impact in the 3D forward GCOAST model framework.

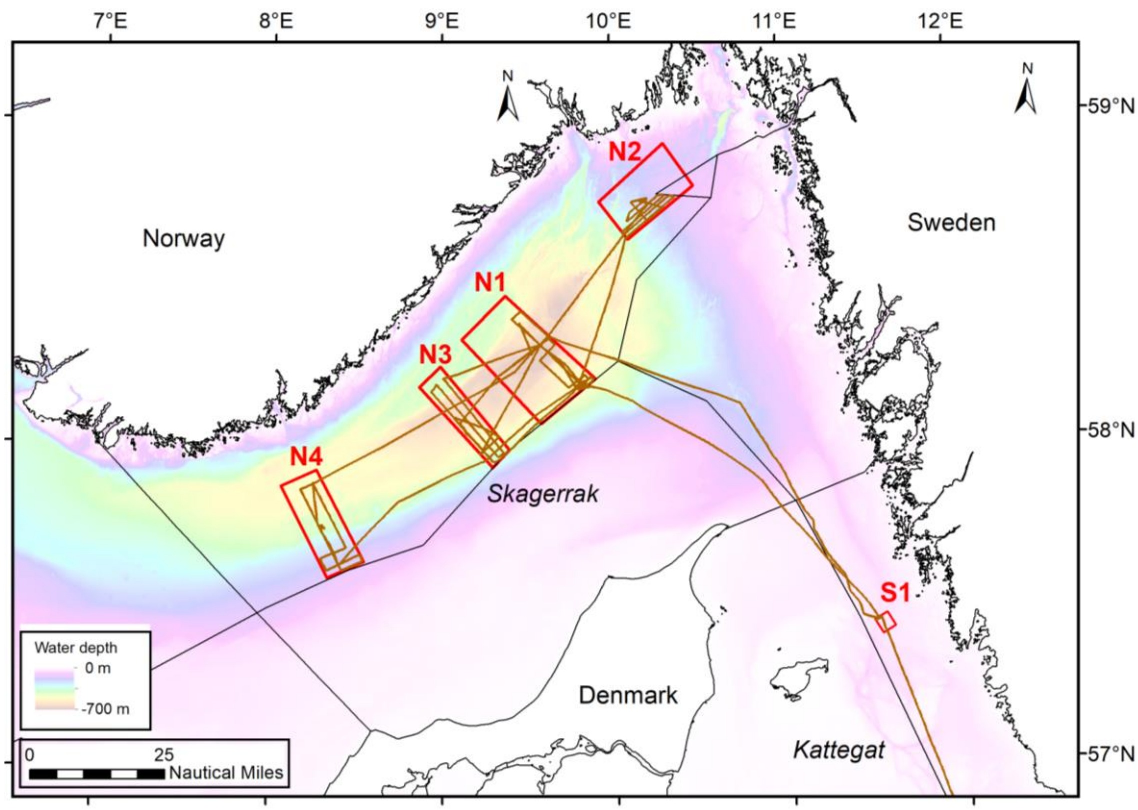


**Fig. 3.2** Track chart (brown line) of RV Alkor cruise AL561 (WGS84/UTM32N projection). Bathymetry from Smith and Sandwell (1997). The five main working areas in Kattegat (S1) and Skagerrak (N1-4) are labelled in red.

# 4 Narrative of the Cruise

In preparation of the AL561 cruise the science crew, with support of GEOMARs' TLZ team and the Alkor crew could successfully load all equipment and build up all analytical devices and sampling equipment on deck of RV Alkor on Friday, July the 30th. Without any delay embarkation started at 8:00 on the following Monday morning (2.8.2021) and RV Alkor left Kiel from GEOMAR, Westufer at 9:00, heading towards Kattegat. Safety introduction was performed during the morning and final tests and routine checks of equipment were finalized until the evening. Sea state was calm and all of us were healthy.

We approached our first sampling area "S1" east of Laeso in the Swedish EEZ at 08:00 on Tuesday the 3rd. A short hydroacoustic survey guided us to the first sediment sampling site. About 60 cm of soft muddy sediment was recovered from there by Multicoring and a busy subsampling program started on deck and in the laboratories. Unfortunately, several attempts to recover the soft sediment by gravity coring failed in the afternoon and we decided to head on towards the Skagerrak. During transit we had to install and program the Lander device to be ready for deployment early next morning. The hydroacoustic survey of N1 was conducted from late in the night of the 3rd of August until morning of the 4th. Additional onsite preparation time of ~4 hours were needed for the Lander station before the Lander was deployed smoothly on the seafloor. Video-CTD hydrocast and sediment sampling was performed in the vicinity of the Lander station until evening of the 4th. During night (4th - 5th) the working area "N2" was partly monitored by hydroacoustic measurements. From 8:00 on until late evening we did perform an exhausting sediment sampling and water column sampling in areas N1 and N2. In general, we established a routine sequence of sediment and water sampling during daytime and hydroacoustic monitoring during night.

After partly monitoring N3 we recovered the first BIGO Lander at 08:00 on Friday the 6th. Sampling of sediment and water from the Lander and sensor data storage worked fine and the Lander was ready to be deployed on the same day late in the evening again. During daytime we performed successful recovery of sediment by gravity- and multi-coring.

Heavy weather was approaching during the night from 6th to 7th when hydroacoustic monitoring was performed in the area N3, our most western area in the Skagerrak. First work on deck was possible at 16:00 again and we could use the MUC for sediment sampling until night. N3 and part of N1 was monitored by echosounders during night again and the second Lander was successfully recovered on Saturday morning the 7th of August. The sea state was fine with 2-3 bf and 1 m wave and decks work was back to our routine schedule with coring followed on Lander recovery and Lander deployment in the evening of the same day, followed by hydroacoustic monitoring during the night. On Monday the 9th we conducted water sampling with the VCTD and sediment sampling with GC and MUC. Tuesday the 10th started with Lander recovery and was followed by MUC and GC coring until 18:00. Final hydroacoustic measurements were performed in the Skagerrak until we had to leave the Norwegian EEZ at 20:30 heading towards our first and last sampling area located in Kattegat (S1).

We reached station S1 late in the night and conducted a short hydroacoustic survey until Wednesday morning when we performed our last station of the AL561 cruise by recovering a 3 m long sediment core. We arrived at Kiel, GEOMAR west-shore on Thursday evening, however, due to logistic reasons we finally rebuild analytical devices and unloaded all equipment on Friday morning the 13th of August.

# 5 Preliminary Results

## 5.1 Hydroacoustic Mapping

(C. Böttner[1])

[1]CAU

### 5.1.1 Innomar Sediment Echosounder

The R/V ALKOR is equipped with a hull-mounted parametric subbottom profiler of type Innomar SES-2000® medium. The subbottom profiler transmits two high frequencies at high sound pressure. These two sound waves interact in the water column, generating harmonics. The SES- 2000® medium sends and records primary frequencies of about 100 kHz and thus generates parametric secondary frequencies within the range of 4 – 15 kHz. Secondary frequencies develop through nonlinear acoustic interaction of the primary waves at high signal amplitudes. The advantage of these secondary frequencies is that they have a similar beam width and short pulse lengths as the primaries despite the low frequency and the small transducer. The system allows a simultaneous acquisition of up to three different frequencies (multi-frequency mode), which are shot sequentially. Every shot records two channels comprising a primary high frequency (HF) and secondary low frequency (LF) as full waveform and envelope. The secondary frequencies are adjustable and were set to 4 kHz with two pulses and 15 kHz with one pulse during all surveys. The system has a vertical resolution of 6 cm and its accuracy depends on the frequency and water depth, e.g. 100/10 kHz: 2/4 cm + 0.02% of the water depth (Wunderlich and Müller, 2003). The soundings are corrected for heave, roll and pitch movements of the vessel. The system worked reliable and produced high-quality data throughout the whole time (Fig. 5.1).

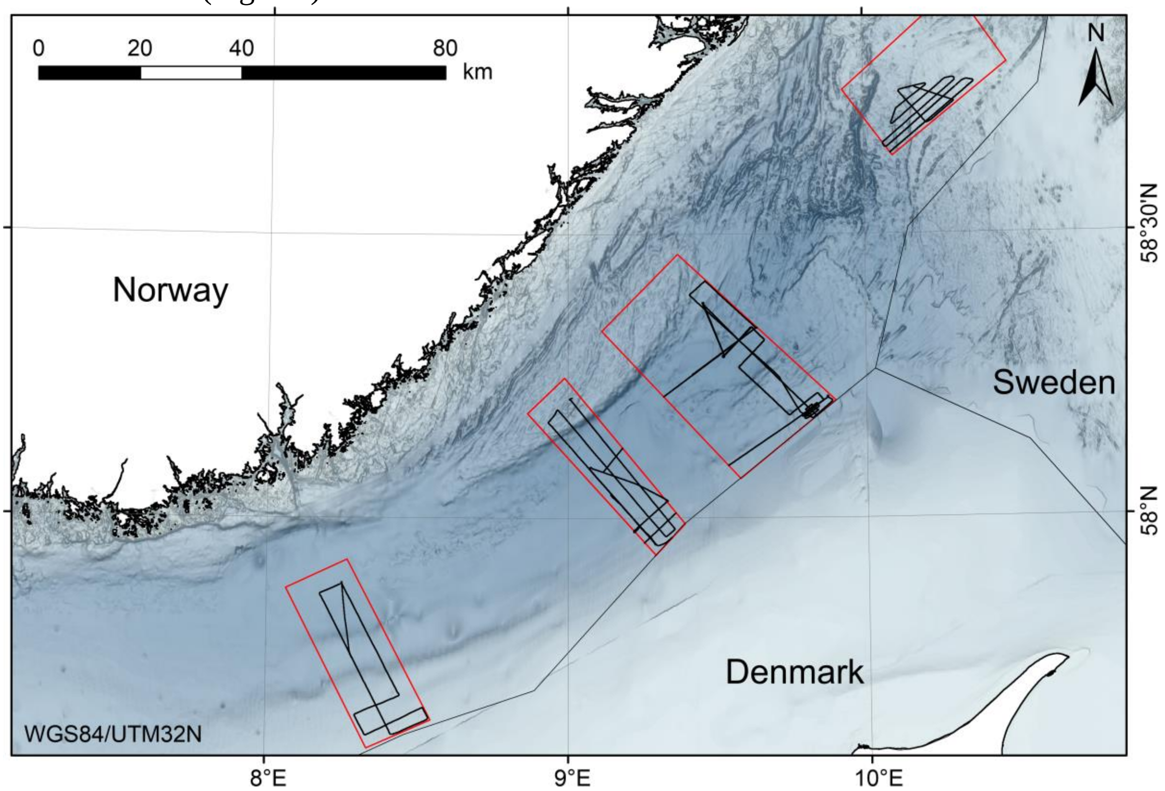


**Fig. 5.1** Bathymetric map of the Skagerrak (EMODnet bathymetry 2020) sowing an overview of all SES profiles in the 4 Norwegian survey areas. In total, we recorded 448 NM of sediment echosounder data.

At the beginning, all profiles were shot with 4 kHz, 2 pulses per ping and high energy mode to achieve high penetration (window length 100 m). During the surveys, the frequency was increased and the system set to 8 kHz, 2 pulses per ping and 100 m window length. However, despite the overall high quality, we encountered problems with the currently outdated software and A/D converter component, diminishing the overall data quality by inducing erroneous pings with z-offsets (with regard to the surrounding seafloor; Fig. 5.2). This error only occurred because of very deep penetration of the system in the Skagerrak and the accordingly large record window length. Innomar was kindly offering remote help and able to identify the error during a remote checkup. The induced noise/error can easily be mitigated by installing software updates and setting up upgraded components (A/D converter).

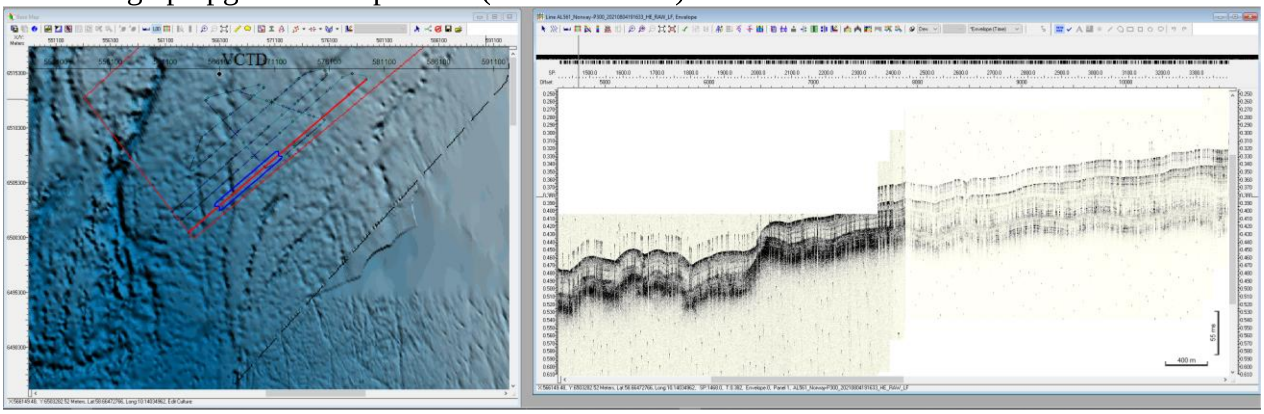


**Fig. 5.2** Screenshot of IHS Kingdom software showing profile AL561_P300 and prominent erroneous pings with z-offsets in the northernmost Norwegian survey area (left map). System was set to 4kHz, 2 pulses, high-energy mode and a window record length of 100 m. In the center of the line (right hand side profile), the window start delay was unfortunately not set to the correct depth interval. This resulted in increasing occurrence of the error. The SES profile shows two-way traveltime in seconds on the y-axis and offset in meter on the x-axis.

After recording, the full waveform data were converted into the segy-format with SES-convert (onboard R/V Alkor). One SEG-Y file was created for the length of each profile, if possible and no changes in settings were applied. We imported the converted segy-files into IHS Kingdom seismic interpretation software and calculated the envelope subsequently.

### Innomar SES2000 medium - Preliminary results

The INNOMAR SES- 2000® medium was mainly used for analysis of the upper sedimentary succession and to identify potential depocenters with presumed high sedimentation rates. The system showed very good penetration depth with very high resolution down to 100 m into the sedimentary column and provided excellent view into the subsurface as well as on sedimentary processes (i.e. contourite body deposition due to local bottom currents).

The sedimentary succession in the survey area is very homogeneous and shows at mostly two major seismo-stratigraphic units. The topmost sediments are characterized by well laminated, relatively low acoustic impedance seismic reflections and show thickness of up to 80 m in some areas, indicating the very high sedimentation rates in this area. These sediment layers show a strong influence of local bottom currents reshaping the seafloor, which is documented by the very pronounced contouritic bodies and/or ubiquitous sedimentary waves. The upper well laminated sediments show a change in impedance likely indicating a transition from glaciomarine to marine sedimentation. The second major stratigraphic unit is the underlying chaotic to transparent body with a corrugated surface likely corresponds to glacial sediments, i.e. glacial till of Pleistocene age (Fig. 5.3).

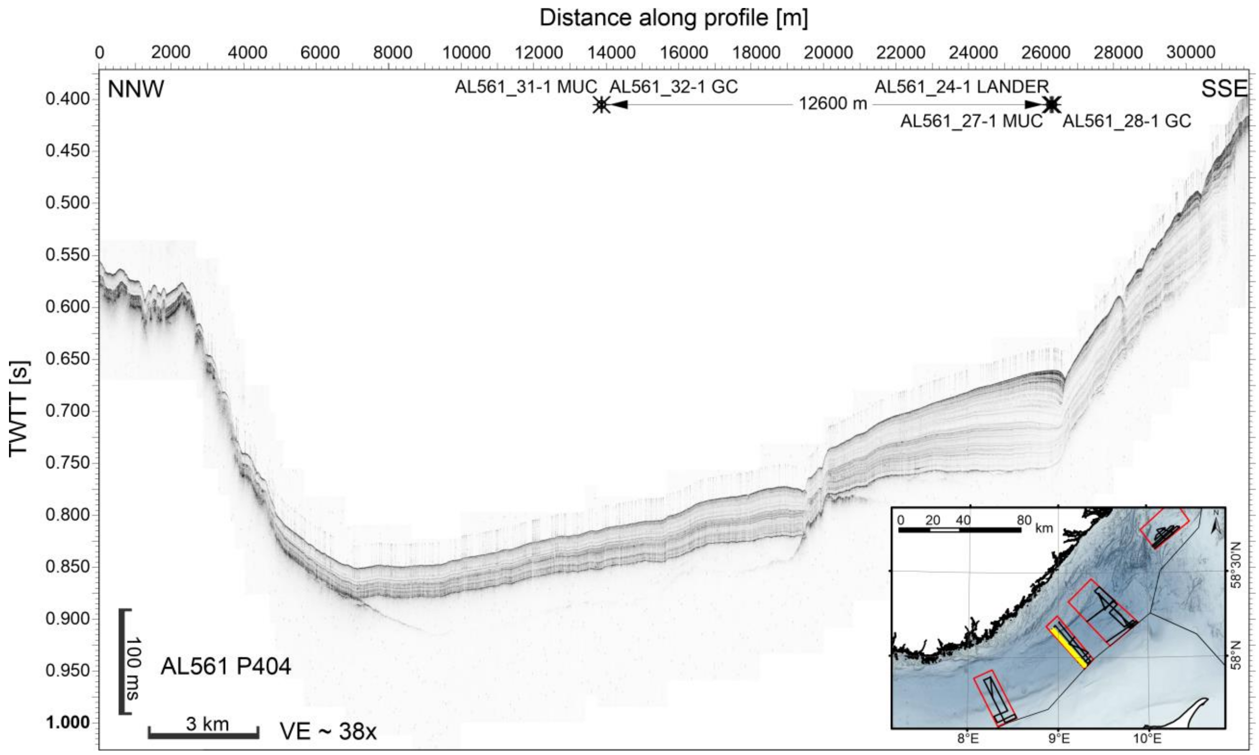


**Fig. 5.3** Innomar SES-2000 medium profile AL561_P404 across the Skagerrak from the Danish border to the Arendal terrace, approximately 12 NM offshore the coast of Norway. The profile shows the very good quality of the data (8 kHz, 2 pulses, 150 m record window length) and very deep penetration of the system. The SES profile shows two-way travel time in seconds on the y-axis and distance along profile in meters on the x-axis.

The parametric sediment echosounder is highly sensitive to free gas in pore space and thus can be used to map shallow gas accumulations. Where free gas exists, usually the amplitudes are damped and blanking of amplitudes occurs beneath the top of the free gas horizon. These free gas areas can be observed at ~14 ms below the seafloor (Fig. 5.4), corresponding to approx. 10 m at 1483 m/s seismic velocity (bulk water sound speed). Blanking seems to occur predominantly towards shallower areas, where free gas also escapes through prominent pockmarks at the seafloor (Laier and Jensen, 2007). However, gas flares in the water column were rarely observed in the shallow parts of the Skagerrak. No indications of free gas inside pore space or the water column were found in the deeper sections of the Skagerrak, where previous publications have identified fields of pockmarks (Hempel et al., 1994; Rise et al., 1999; Longva et al., 2009). Pockmarks are circular to semi-circular depressions of the seafloor and indicate the flux of fluids (i.e. gases and liquids) from the subsurface. The absence of free gas in the upper sedimentary succession evidences that the responsible fluids for pockmark formation must be sourced from deeper parts of the sedimentary succession (Rise et al., 1999).

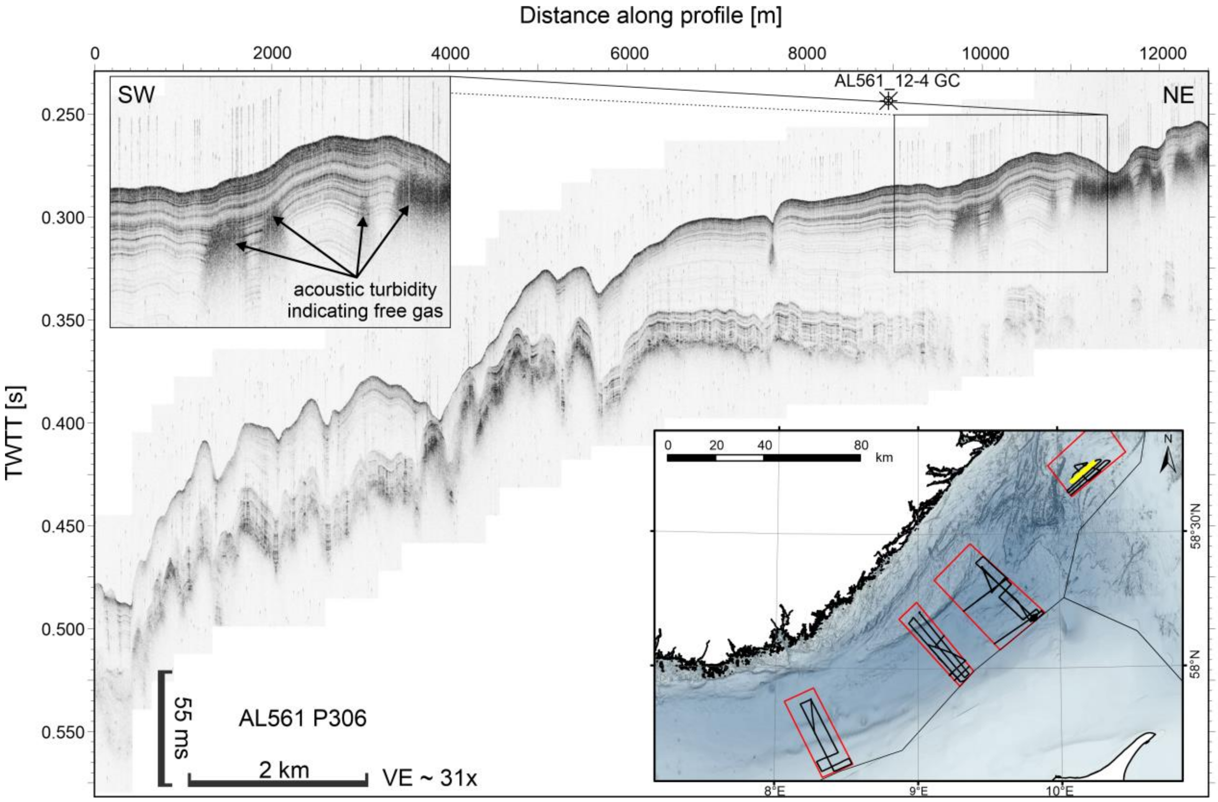


**Fig. 5.4** Innomar SES-2000 medium profile AL561_P306 across the northernmost survey area outside the Oslo fjord, approximately 12 NM offshore the coast of Norway. The profile shows pronounced acoustic turbidity crosscutting the overall stratification, indicating free gas inside pore space. The majority of gas seems to be located in approx. 10 m below the seafloor (calculated from 14 ms at 1483 m/s seismic velocity), while it reaches the seafloor in only few places (i.e. pockmarks or troughs). The SES profile shows two-way travel time in seconds on the y-axis and distance along profile in meters on the x-axis.

### 5.1.2 EK 60 fishery echosounder

The hull-mounted fishery echosounder KONGSBERG EK60 was operated with all frequencies (38, 70, 120, and 200 kHz) for gas bubble flare imaging. Pulse length and power were set constant throughout the cruise. The system was operated simultaneously to the Innomar SES-2000 medium.

### EK60 Preliminary Results

Very few gas seep locations could be identified and rise heights were mapped. The few gas seeps were found close to the Danish border (Fig. 5.5**Fig**) or close to the Norwegian coastline in the northernmost survey area. The surveys were not dedicated to gas emission estimation and thus shows dominant reoccurring noise superposing the water column imaging. The imaging shows prominent layers in the upper water column indicating that in combination with CTD data the system could be used for water mass identification (hydroacoustic oceanography).

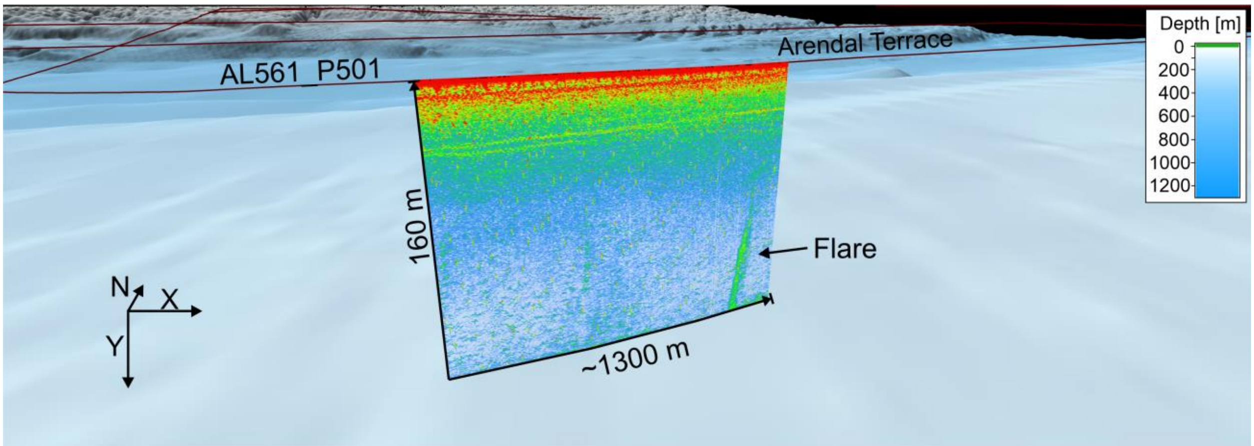


**Fig. 5.5** Hydroacoustic profile AL561 P501 with the first channel (38kHz) of the EK60 fishery echosounder. The profile shows one of the very few gas flares in the water column, indicating gas release from the seafloor. The gas flare is visible to approx. 100 m above the seafloor. The image is facing northwards to the Norwegian coastline and the Arendal Terrace.

## 5.2 Water and Sediment sampling

### 5.2.1 In situ benthic flux measurements using the BIGO type Lander (Biogeochemical Observatory)

(S. Sommer[1], A. Dale[1], B. Domeyer[1], A. Petersen[1], R. Surberg[1], M. Türk[1])

[1]GEOMAR

Major goal was to quantify the current in situ magnitude of particulate organic carbon (POC) turnover in sediment and fluxes of associated elements across the sediment water interface in the deep northeastern Skagerrak (North Sea) in water depths of 490 to 677 m. This region represents a major depo-center for POC originating from the North Sea with sedimentation rates of up to 11 mm $yr^{-1}$ and organic carbon contents of 3 wt-% (for references see introduction). The Skagerrak is considered to be a net sink for organic carbon (Ståhl et al. 2004), where burial and storage of POC constitutes a major $CO_2$ removal capacity. The results of the flux measurements will be linked to the geochemistry of sediments obtained by the Multiple- and the Gravity Corer and will contribute to apply a model framework to simulate current, past and future POC cycling and to identify human pressures affecting the turnover and burial of POC in the North Sea.

In situ fluxes of primarily oxygen ($O_2$) as well as dissolved inorganic carbon (DIC), total alkalinity (TA), nitrate ($NO_3^-$), nitrite ($NO_2^-$), ammonium ($NH_4^+$), phosphate ($PO_4^{3-}$) and silicic acid ($H_4SiO_4$) across the sediment water interface were determined to study carbon cycling and that of associated major elements. Furthermore, additional ICP and IC measurements were conducted.

Three BIGO deployments were conducted at the main stations N1 and N3 Table 5.1.

**Table 5.1** Details of the lander deployments.

| Date/time (UTC) | station | deployment | area | latitude N | longitude E | depth (m) |
|---|---|---|---|---|---|---|
| 04.08.21 08:40 | 5 | BIGO-II-1 | N1 | 58°10.980’ | 09°47.230’ | 502 |
| 06.08.21 14:55 | 17 | BIGO-II-2 | N1 | 58°18.784’ | 09°34.337’ | 677 |
| 06.08.21 14:55 | 24 | BIGO-II-3 | N3 | 57°59.233’ | 09°14.302’ | 490 |

For the measurement of solute fluxes in combination with sediment retrieval BIGO-II was deployed as described in detail by Sommer et al. (2009), Fig. 5.6a, b. In brief, BIGO-II contained two circular flux chambers (internal diameter 28.8 cm area 651.4 $cm^2$). A TV-guided launching system allowed smooth placement of the observatory at the sea floor. About 2.25 hours (BIGO-II-1) or 4.25 hours (BIGO-II-2/3) after the observatories were placed on the seabed the chambers were slowly driven into the sediment (~ 30 cm $h^{-1}$). During this initial time period, where the bottom of the chambers was not closed by the sediment, the water inside the flux chamber was periodically replaced with ambient bottom water. The water body inside the chamber was replaced once more with ambient bottom water after the chamber has been driven into the sediment to flush out solutes that might have been released from the sediment during chamber insertion. To trace solute fluxes ($NO_3^-$, $NO_2^-$, $NH_4^+$, $PO_4^{3-}$, $H_4SiO_4$) sequential water samples were removed with glass syringes (volume ~ 47 ml) by means of syringe water samplers, Fig. 5.6. These water samples are further used for the ICP- and IC-analyses.

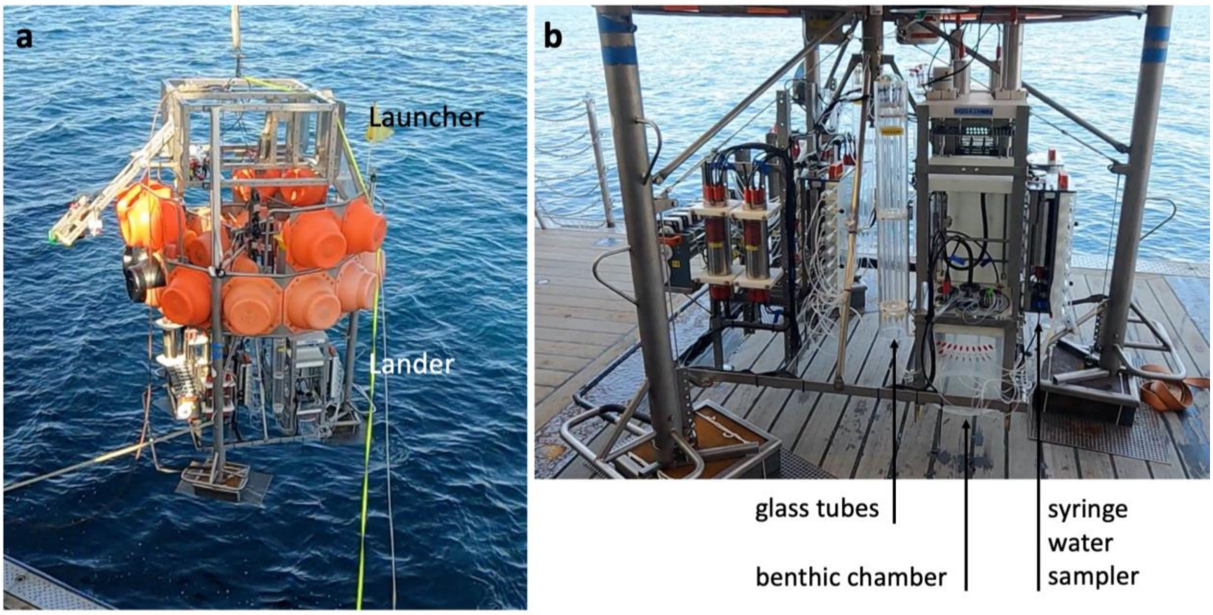


**Fig. 5.6** a. Launching unit mounted on top of the lander; b. details of the benthic flux chamber and the water sampling systems (syringe water sampler, glass tube for the sampling of undiluted water samples using an 8-channel peristaltic pump).

The syringes were connected to the chamber using 1 m long Vygon tubes with a dead volume of 5.2 ml. Prior to deployment these tubes were filled with distilled water. Another 8 undiluted water samples were taken from inside each of the two benthic chambers using an eight-channel peristaltic pump, which slowly filled glass tubes (quartz glass), Fig. 5.6b. These samples will be

used for the gas analyses of DIC, TA and iron. To monitor the ambient bottom water geochemistry an additional syringe water sampler and another series of eight glass tubes were used. The positions of the sampling ports were placed about 40 to 50 cm above the sediment water interface. Oxygen was measured inside the chambers and in the ambient seawater using optodes (Aandera). They were two point calibrated before each lander deployment using well oxygenated seawater and anoxic seawater, which was produced using 5 to 15 g sodium sulfite. Upon retrieval of the BIGO-II onboard, the water samples were stored in the cool room until subsampling and further processing. The syringe water samples were transferred into Zinser vials, from which subsamples were taken to measure $PO_4^{3-}$ and $H_4SO_4$ onboard. The remaining fraction was frozen and will be analyzed at the GEOMAR laboratories using an auto-analyzer. The water samples for DIC and total alkalinity analysis were taken according to the slightly modified Standard Operation Procedures described by Dickson et al. (2007). The water samples obtained in the glass tubes were transferred into Pyrex test tubes (volume: 14 ml). Subsequently a small headspace was applied removing 3.4 ml of the water sample, which was dispensed into Zinser vials containing acid for later iron analysis. The resulting headspaces in the Pyrex test tubes were variable, since the volume of the glass tubes was variable and in some cases not enough sample volume was available to completely fill the Pyrex test tubes. After headspace application, the samples were poisoned with 20µl of mercury chloride solution using an Eppendorf Vario pipette. The test tubes were closed using greased (Wacker Silicone Grease P4) glass stoppers, which were secured using plastic clamps and stored in the cool room.
Short sediment cores including a small amount of bottom water from each flux chamber was taken using Perspex liners with 10 cm inner diameter. The sediment cores were directly sliced on board for the geochemical analysis of $NO_3^-$, $NO_2^-$, $NH_4^+$, $PO_4^{3-}$, $H_4SiO_4$, total alkalinity, DIC, ICP-MS, IC, water content, porosity and C/N elemental ratios.

**Preliminary Results**

The envisaged three lander deployments were successfully conducted in the deeper part of the Skagerrak (Areas N1 and N3; Fig. 3.2). During all lander deployments, the sediments were retrieved fully intact by the benthic flux chambers. Except for deployment BIGO-II-3, indications for sediment disturbance caused by the lander were not observed. During deployment BIGO-II-3 a small area (< 10 % of the chamber area) displayed a slightly disturbed sediment surface. During the deployments BIGO-II-2 and BIGO-II-3 abundant vermiform organisms were noticed, which most likely represent frenulate tube worms. Small frenulate pogonophorans have been reported from shelf and slope environments of the northeastern Atlantic including the Skagerrak (Dando et al. 2008, Flügel & Langhof, 1982, Kirkegaard 1958). Typically, they occur in muddy, organic rich sediments and rely for their nutrition on endosymbiotic bacteria that take up reduced sulfur species. In contrast to the deployments of BIGO-II-1 and BIGO-II-2, during the third deployment indications (holes at the sediment surface) for intense bioturbation were not discerned.
The incubation period at the seabed and the volume of the overlying water column inside the benthic chambers are given in table 5.2. The specific times of sampling during each lander deployment is given in the Appendix (Tab. A12.1). The time course of oxygen consumption during the different lander deployments for each benthic chamber is depicted in figure 5.7.

**Table 5.2** Preliminary oxygen, $PO_4^{3-}$ and $H_4SiO_4$ fluxes (mmol $m^{-2}$ $d^{-1}$), incubation period defined as the time span between synchronized chamber insertion and final syringe sampling (h), volume of the overlying bottom water enclosed by the flux chamber (l), curve fit used for fitting the oxygen concentrations. The concentrations of $PO_4^{3-}$ and $H_4SiO_4$ were linearly fitted. For the calculation of the organic carbon degradation rate ($C_{org}$ deg.) see main text. C/P denotes the ratio between organic carbon degradation and phosphate release. Please note that $PO_4^{3-}$ and $H_4SiO_4$ will be again measured at GEOMAR laboratories.

| deployment | chamber | oxygen | BW $O_2$ | incubation | volume | fit type |
|---|---|---|---|---|---|---|
| BIGO-II-1 | Ch1 | -5.2 | BIGO-II-1 | 35.75 | 13.024 | exponential |
| | Ch2 | -4.6 | | 35.75 | 13.342 | linear |
| BIGO-II-2 | Ch1 | -5.0 | BIGO-II-2 | 28.75 | 14.755 | double exp. |
| | Ch2 | -7.3 | | 28.75 | 12.918 | double exp. |
| BIGO-II-3 | Ch1 | -6.9 | BIGO-II-3 | 28.75 | 13.059 | double exp. |
| | Ch2 | -5.6 | | 28.75 | 14.102 | double exp. |

| deployment | chamber | phosphate | silicic acid | $C_{org}$ deg. | $C_{org}/PO_4^{3-}$ |
|---|---|---|---|---|---|
| BIGO-II-1 | Ch1 | 0.04 | 1.16 | 3.59 | 90 |
| | Ch2 | 0.03 | 1.29 | 3.17 | 106 |
| BIGO-II-2 | Ch1 | 0.05 | 0.47 | 3.45 | 69 |
| | Ch2 | 0.06 | 1.90 | 5.03 | 84 |
| BIGO-II-3 | Ch1 | 0.06 | 1.58 | 4.76 | 79 |
| | Ch2 | 0.05 | 1.55 | 3.86 | 77 |

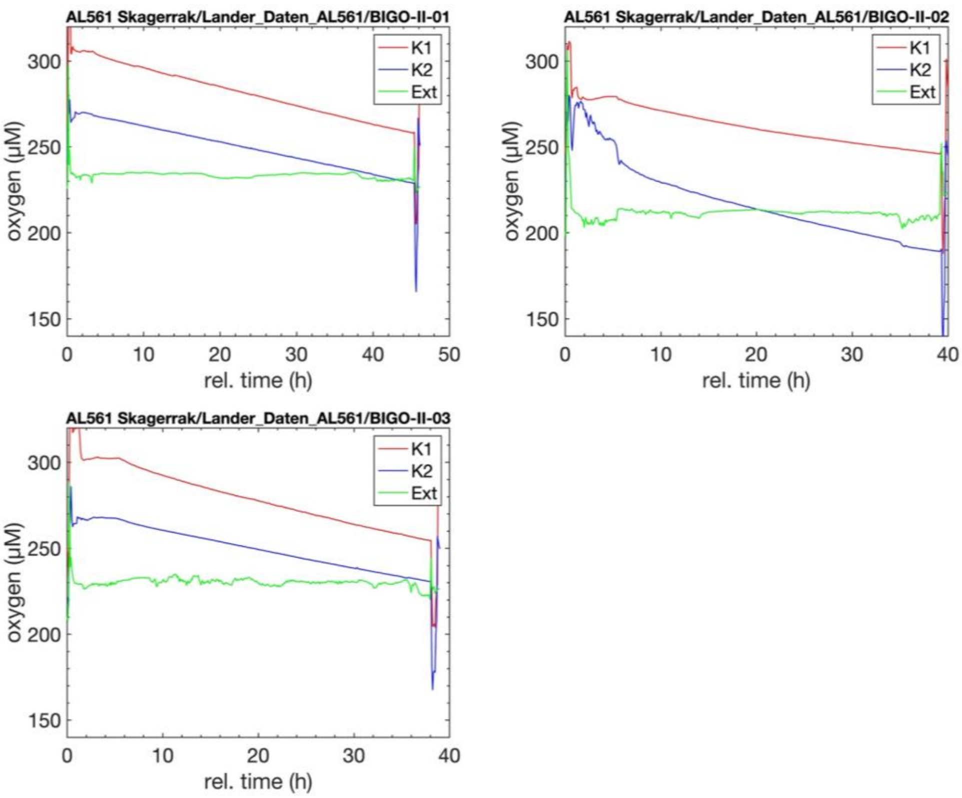


**Fig. 5.7** Time course of the oxygen concentration inside the benthic chambers K1 (Chamber 1) and K2 (Chamber 2) in comparison to the ambient bottom water (Ext) during all lander deployments.

The oxygen fluxes measured at the three different locations comprising a depth range of 490 to 677 m were similar to each other and ranged between -4.6 and -7.3 mmol $m^{-2}$ $d^{-1}$.
In the Skagerrak at water depths of 356 and 562 m Ståhl et al. (2004, their stations H3 and T2) determined in-situ oxygen fluxes of -4.7 as well as -1.9, -7.2 and -24.8 mmol $m^{-2}$ $d^{-1}$ respectively. In an earlier study (Bakker & Helder, 1993) diffusive oxygen fluxes in the range of -2.6 to -17.9 mmol $m^{-2}$ $d^{-1}$ at water depths of 528 to 677 m were determined using needle and micro electrodes. Using a molar ratio between oxygen consumption and carbon degradation of 1.45 (Hedges et al., 2002) and neglecting oxygen consumption during nitrification preliminary aerobic degradation rates between 3.2 and 5.0 mmol $m^{-2}$ $d^{-1}$ were calculated.
Onboard measurements of $PO_4^{3-}$ and $H_4SiO_4$ revealed a release of both solutes. $PO_4^{3-}$-release was very low and ranges between 0.03 and 0.06 mmol $m^{-2}$ $d^{-1}$. The ratio between organic carbon degradation and $PO_4^{3-}$-release at the different stations comprises a range of 69 to 106 indicating increased $PO_4^{3-}$ release in comparison to Redfield stoichiometry. Fluxes of $H_4SiO_4$ were in between 0.5 and 1.9 mmol $m^{-2}$ $d^{-1}$. During ex situ nutrient flux measurements in the Skagerrak in 1991 - 1994 (water depths: 482 – 682 m) using sediment cores obtained by a multiple corer, $PO_4^{3-}$ and $H_4SiO_4$ fluxes in the range of 0.01 to 0.1 and 0.6 to 2.1 mmol $m^{-2}$ $d^{-1}$ were determined (Hall et al. 1996).
These flux measurements will contribute to constrain the current POC cycling and burial of POC in the deep Skagerrak. Next steps will be to finalize the geochemical analysis of the water- and sediment samples at the GEOMAR laboratories.

### 5.2.2 Sediment and Porewater Geochemistry

(T. Spiegel[1], N. Lenz[1], B. Domeyer[1], R. Surberg[1], A. W. Dale[1])
[1]GEOMAR

Sediment and pore water samples were taken at eight locations in the working area of Skagerrak and Kattegat. The object is to establish a high-resolution age-depth model to quantify the lateral export of sediments and particulate organic carbon (POC) in the past 200 years. The overarching goal is to understand how the cycling of POC contributes to carbon sequestration in the North Sea and how this system is influenced by anthropogenic effects including fisheries, resource extraction, sediment management and eutrophication. At a later stage, the sediment and porewater chemistry as well as the precise age dating will be coupled to a numerical reaction transport model to reconstruct historical POC variations at the seafloor and constrain lateral POC transport under changing environmental conditions. This summary reports on the porewater geochemistry measurements that were made during the cruise.

An overview of the sediment sampling stations is given in Table 5.3. Sediment cores were mainly retrieved using a multiple-corer (MUC) and gravity corer (GC) (Fig. 5.8). Sediments were also recovered in each benthic chamber of the BIGO lander (Fig. 5.6).

The MUC was equipped with seven, 60 cm long, Perspex liners with an internal diameter of 10 cm. The MUC was lowered into the sediment with a speed of 0.3 m $s^{-1}$ in all deployments. Once on the seafloor, the liners were pushed into the sediment under gravity by a set of lead weights. Penetration always exceeded 30 cm due to the soft nature of the sediment. BIGO cores were taken by pushing the short liners (diameter 10 cm, length ca. 20 cm) into the sediment within the incubation chambers once the BIGO was on deck. After retrieval, all cores were transferred to a refrigerated laboratory adjusted to the bottom water temperature (ca. 7-8°C) and processed immediately. Supernatant bottom water of the MUC and BIGO cores was sampled and filtered for subsequent analyses.

The GC was equipped with a 3 m long core barrel and 4 additional lead weights (a 50 kg) were used (gross weight ~350 kg). It was lowered into the sediment with a rope speed of 0.8 m $s^{-1}$ resulting in core recovery of ~ 3m. After the GC was on deck, the inner plastic liner (inner diameter of 11 cm) was pulled out and cut into 1-m long segments that were subsequently cut lengthwise to yield a sampling half and an archive half. Geological core description and sediment photography was followed by sediment sampling for geochemical analyses. Subsequently, the sampling and archive halves were transferred into labelled D-tubes for long-term storage at 4°C in the refrigerated core repository at GEOMAR.

For sub-sampling and measurement of redox-sensitive parameters (e.g. dissolved Fe, nutrients) in the MUC cores, the sediments were sectioned inside an argon-filled glove bag and filled into 50 ml Falcon tubes. The sampling depth resolution increased from 1 cm at the surface to 4 cm at larger depths. Sediment samples were then spun in a refrigerated centrifuge at 4000 G for 20 min at 8 $^{o}$C to separate the porewater from the particulates. Subsequently, the porewater samples were filtered (0.2 µm cellulose-acetate syringe filters) inside the glove bag.

BIGO core porewater distributions are subject to artefacts from being incubated on the seafloor for up to 36 h, potentially leading to alterations to the surface concentration gradients. Thus, only a limited number of parameters were analysed in the BIGO cores to check for overall consistency with MUC data. This allows the BIGO fluxes to be linked with the MUC data that are less prone to disturbances. BIGO cores were rapidly sectioned under ambient atmosphere.

For both MUC and BIGO cores, ~10-30 ml porewater were extracted at each depth interval. Sediment samples for determining water content and solid phase constituents at GEOMAR were taken from a different sediment core from the same MUC deployment.

For the GCs, porewater was extracted from the sampling halves by inserting rhizones into the sediment (type CCS from Rhizosphere with a pore size of 0.15 µm). The first 0.5 ml of porewater extruded was discarded. Porewater extraction using this method required up to 2 hr, yielding 5-10 ml of porewater at each depth interval.

A total of 422 porewater samples were analyzed on board (Table 5.3). The following solutes were determined: total dissolved ammonium ($NH_4^+$), total dissolved phosphate ($PO_4^{3-}$), total dissolved silicate ($H_4SiO_4$) and total alkalinity (TA). $NH_4^+$, $PO_4^{3-}$, and $H_4SiO_4$ were determined using standard methods (Grasshoff et al., 1997) on a Hitachi U-2001 spectrophotometer, i.e. $NH_4^+$ as indophenol blue, $PO_4^{3-}$ and $H_4SiO_4$ as molybdenum blue. The precision of the analysis for $NH_4^+$, $PO_4^{3-}$, and $H_4SiO_4$ was 1 µmol $L^{-1}$, 1 µmol $L^{-1}$ and 5 µmol $L^{-1}$, respectively. Samples for nitrate ($NO_3^-$) and nitrite ($NO_2^-$) were frozen (-20 $^{o}$C) for later analysis. Nutrient samples from the BIGO syringe samples were dealt with in the same way. TA was analyzed by titration of 0.25-1 ml pore water according to Ivanenkov and Lyakhin (1978) with an analytical precision of 0.05 meq $L^{-1}$. Titration was ended when a stable pink colour appeared. During titration, the sample was degassed by continuously bubbling nitrogen to remove any generated $CO_2$ and $H_2S$. The procedure was standardized using an IAPSO seawater solution.

Sub-samples (4-5 ml) of porewater from the MUCs were acidified inside the glove bag with suprapure concentrated $HNO_3^-$ (10 µl per ml of sample) for analysis of total dissolved iron, major elements (K, Li, B, Mg, Ca, Sr, Mn) and trace elements by inductively coupled plasma optical emission spectroscopy (ICP-OES) at GEOMAR. Untreated samples were also stored refrigerated for onshore analysis of $Cl^-$, $Br^-$, and $SO_4^{2-}$ by ion-chromatography. Dissolved inorganic carbon will be determined on selected samples at GEOMAR.

From the MUCs and GCs, 3 ml of sediment were taken with a syringe and transferred into 20-ml headspace vials filled with 6 ml of a saturated NaCl solution for onshore gas chromatographic analysis of dissolved methane and higher hydrocarbons.

Sediment sub-samples were taken every 1 cm from the MUCs for onshore analyses of clay minerals and isotope ratios of radiogenic elements ($^{87}Sr/^{86}Sr$, $^{176}Hf/^{177}Hf$ and $^{143}Nd/^{144}Nd$). The elemental and isotopic composition of detrital sediments will be used to infer changes in the provenance of sediments deposited in the Skagerrak. An additional MUC core was sub-sampled at the same resolution for onshore analyses of $^{210}Pb$ and $^{134}Cs$ to create a high-resolution age model over the last 100 – 200 years. These sediments were all refrigerated on board.


a


b

**Fig. 5.8** a. Multicorer equipped with 7 plastic liners, online camera and light; b. Gravity corer with 3 m tube operated at low sea-state.

**Table 5.3** Sampling details for sediment geochemistry organized by date.

| Date | Station/Gear [a] | Site | Depth (m) | Latitude N | Longitude E | Method[b] | Geochem. | Methane | Phys. Props. | $^{210}$Pb | Provenance |
|---|---|---|---|---|---|---|---|---|---|---|---|
| 02. Aug 21 | 2MUC1 | S1 | 65 | 57° 27.030' | 11° 30.480' | Under argon | x | x | x | x | x |
| 04. Aug 21 | 5BIGO2-1 K1 | N1 | 502 | 58° 10.975' | 9° 47.239' | Under air | x | | x | | |
| 04. Aug 21 | 5BIGO2-1 K2 | N1 | 502 | 58° 10.975' | 9° 47.239' | Under air | x | | x | | |
| 04. Aug 21 | 7MUC2 | N1 | 500 | 58° 10.884' | 9° 47.624' | Under argon | x | x | x | x | x |
| 05. Aug 21 | 11MUC3 | N2 | 215 | 58° 44.876' | 10° 13.437' | Under argon | x | x | x | x | x |
| 05. Aug 21 | 12GC4 | N2 | 214 | 58° 44.878' | 10° 13.447' | Rhizones | x | x | x | | |
| 06. Aug 21 | 16GC5 | N1 | 492 | 58° 10.891' | 9° 47.566' | Rhizones | x | x | x | | |
| 06. Aug 21 | 17BIGO2-2 K1 | N1 | 678 | 58° 18.778' | 9° 34.362' | Under air | x | | x | | |
| 06. Aug 21 | 17BIGO2-2 K2 | N1 | 678 | 58° 18.778' | 9° 34.362' | Under air | x | | x | | |
| 07. Aug 21 | 19MUC5 | N4 | 434 | 57° 45.191' | 8° 17.173' | Under argon | x | x | x | x | x |

| | | | | | | | | | | | |
|---|---|---|---|---|---|---|---|---|---|---|---|
| 07. Aug 21 | 20MUC6 | N4 | 185 | 57° 38.086' | 8° 23.998' | Under argon | x | x | x | x | x |
| 08. Aug 21 | 22MUC7 | N1 | 677 | 58° 18.785' | 9° 34.335' | Under argon | x | x | x | x | x |
| 08. Aug 21 | 24BIGO2-3 K1 | N3 | 490 | 57° 59.220' | 9° 14.300' | Under air | x | | x | | |
| 08. Aug 21 | 24BIGO2-3 K2 | N3 | 490 | 57° 59.220' | 9° 14.300' | Under air | x | | x | | |
| 09. Aug 21 | 27MUC8 | N3 | 490 | 57° 59.286' | 9° 14.305' | Under argon | x | x | x | x | x |
| 09. Aug 21 | 28GC7 | N3 | 490 | 57° 59.275' | 9° 14.362' | Rhizones | x | x | x | | |
| 10. Aug 21 | 31MUC9 | N3 | 604 | 58° 04.352' | 9° 5.736' | Under argon | x | x | x | x | x |
| 10. Aug 21 | 32GC8 | N3 | 604 | 58° 04.348' | 9° 5.743' | Rhizones | x | x | x | | |
| 11. Aug 21 | 34GC9 | S1 | 66 | 57° 27.021' | 11° 30.492' | Rhizones | x | x | x | | |

[a] K1 and K2 refer to chamber 1 and chamber 2 on the BIGO lander.

[b] Sediments were sectioned either under argon inside a glove bag (MUC), under air (BIGO), or else rhizones were used to extract porewater (GC)

**Preliminary Results**

An illustrative example of porewater data from the sampling sites are shown for a location in the region "N3" in Fig. 3.2. Similar trends were observed at the other sites. TA, $NH_4^+$, $PO_4^{3-}$, and $H_4SiO_4$ all increased with depth in the sediment due to the ongoing remineralization of organic matter. TA, $NH_4^+$ and $PO_4^{3-}$ increased gradually to ~130 cm, whereas $H_4SiO_4$ showed a stronger enrichment in the surface layer, reaching 400 µM by 50 cm depth. All parameters displayed a steepening of the concentration gradient at ~130 cm, which is indicative of an increase in the intensity of organic matter remineralization. Over the whole sediment depth, TA, $NH_4^+$, $PO_4^{3-}$, and $H_4SiO_4$ varied from 2.3 - 20 mM, 2 - 1550 µM, 1.3 - 160 µM and 20 - 460 µM, respectively, at this site. Alignment of the MUC and GC data suggest that around 20 cm of sediment may have been lost during penetration of the GC into the seafloor. This will be determined more accurately when other major ion data have been measured.

Previous work in the Skagerrak suggests that organic remineralization in the long sediment cores studied here will most likely be coupled to sulfate reduction and methanogenesis (Knab et al., 2009; Dale et al., 2009). In organic-rich coastal sediments, aerobic respiration and denitrification will be confined to the upper few centimeters (Devol and Christensen, 1993). The regression slope of a plot of $NH_4^+$ versus $PO_4^{3-}$ concentrations from this site is approximately 9.3 (not shown). Correcting this for the ratio of the bulk molecular diffusion coefficients (D) at in situ temperature and pressure ($D_{NH4}$ = 396 cm$^2$ yr$^{-1}$; $D_{PO4}$ = 146 cm$^2$ yr$^{-1}$) gives a N:P remineralization ratio of 25. This is almost twice as high as the Redfield ratio of 16, presumably due to loss of P into authigenic minerals or $PO_4^{3-}$ adsorption onto Fe oxides (Ruttenberg and Berner, 1993). Similarly, the regression slope of a plot of $NH_4^+$ versus TA concentrations is approximately 0.091, which gives a N:TA remineralization ratio of 0.16. For remineralization of organic matter with a zero oxidation state, the expected N:TA remineralization ratio for sediment dominated by sulfate reduction and methanogenesis is 0.13 and 1.1, respectively (Dale et al., 2021). This preliminary analysis, therefore, demonstrates that sulfate reduction is expected to be the major carbon oxidation pathway in the Skagerrak cores. Sulfate data will show this more clearly when the data become available.

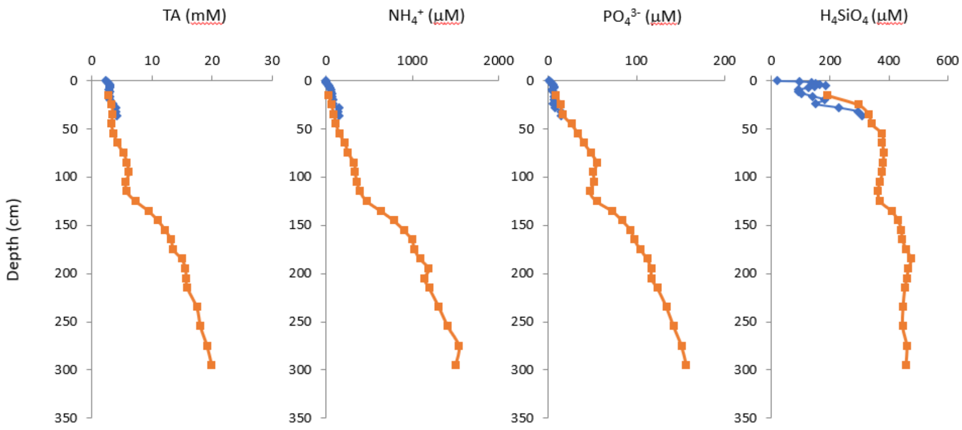


**Fig. 5.9** Dissolved concentrations of TA, $NH_4^+$, $PO_4^{3-}$, and $H_4SiO_4$ measured in cores MUC9 (blue curves) and GC8 (orange curves) taken in close proximity to each other in the region "N3". The GC data have been shifted upwards by 20 cm to compensate for loss of surface sediment.

### 5.2.3 Water Sampling with Video-CTD/Rosette and Onboard Filtration

(N. Lenz[1], T. Spiegel[1], B. Domeyer[1], R. Surberg[1], A. W. Dale[1], M. Schmidt[1])

[1]GEOMAR

A Video-CTD (VCTD) system constructed in a stainless steel Niskin bottles rosette was operated to collect oceanographic data and water samples (Fig. 5.10). Basically, the Video-CTD device was equipped according to Linke et al., 2015. The SBE 9plus underwater unit operated two pressure sensors, 2 temperature sensors, 2 oxygen sensors and 2 conductivity sensors. Furthermore, a Wetlabs sensor measuring turbidity and chlorophyll-a, and an altimeter were attached. The SBE underwater unit and Niskin bottle carousel motor were powered via the winch's coaxial-cable by using the modem/power unit from SST (Linke et al., 2015). Niskin bottle 1 was replaced by a CONTROS methane sensor (HydroC-CH4M). The external $CH_4$-sensor was powered by 24 V battery packs, which were attached to the steel frame. The digital video and data telemetry system (Linke et al., 2015) providing real-time monitoring of the seafloor was also used to control the distance to the seafloor in "bottom view" mode.

VCTD data recording and triggering Niskin bottles was controlled with SEASAVE software (version 7.21) on an external laptop. CTD data were recorded with 24 Hz. GPS position data was logged parallel to the CTD data from NMEA-string of RV Alkor. Hydro-casts and hydrographic data from CTD casts were processed by using SBE software SBE7.22.1. Usually data files of 1 minute bins and 1 meter bins were created from raw data files and exported to ASCII. CTD data is combined with data sets from external sensors by correlating with their UTC time stamps.

The 4 VCTD hydrocasts were carried out at stations in the Skagerrak (Tab. 5.4), where also benthic lander data, MUC and GC samples were recovered. Bottom water (5m above ground) and selected water column samples were taken where maxima of turbidity and chlorophyll-a was measured. The respective suspended particulate matter (SPM) was sampled from Niskin bottles onboard by using suction filtration. 1-liter seawater was filtered for each parameter on pre-combusted Whatmen glass fiber filters (44 mm, 0.7 µm) using a vacuum suction device (Fig.

5.11). For every parameter and depth, duplicate filtrations were carried out. After filtration, filters were wrapped in Al-foil and stored in liquid nitrogen for subsequent onshore laboratory analyses. Bottom water and surface water samples were also taken for onshore analyses of the neodymium seawater composition from the authigenic fraction (Mn-Fe-coatings of particles and foraminifera). The neodymium signal of the seawater helps to reconstruct the seawater circulation of the Skagerrak.

**Table 5.4:** Stations at which the VCTD hydrocasts were carried out during AL561

| Date | Station | Site | Latitude [N] | Longitude [E] | Water depth [m] |
|---|---|---|---|---|---|
| 04-08-2021 | 6 VCTD1 | N1 | 58° 10,884' | 009° 47,611' | 500 |
| 05-08-2021 | 13 VCTD2 | N1 | 58° 18,782' | 009° 34,362' | 694 |
| 09-08-2021 | 25 VCTD3 | N3 | 57° 59,305' | 009° 14,291' | 490 |
| 09-08-2021 | 26 VCTD4 | N3 | 57° 59,279' | 009° 14,296' | 490 |

**Fig. 5.10** Video-CTD device operated on RV Alkor with winch 1 (11 mm coaxial cable).

**Fig. 5.11** Vacuum suction device for filtration of particulate matter suspended in Niskin water samples. A vacuum level in the barrel of about 900 mbar is controlled by the inlet valve on top of the barrel.

## Preliminary Results

4 VCTD hydrocasts were conducted in the main depocenter area of the Skagerrak (Areas N1 and N2; Fig. 3.2). Maximum water depths between ~490 and 690 mbsl were reached during hydrocasts (Tab. 5.4; Fig. 5.12). Surface water temperatures of about 17°C and salinity of about 31 change to temperatures and salinity data of about 7-8°C and 35, below 50 m water depth (Fig. 5.12). Chlorophyll-a and oxygen maxima in the upper 50 m of the water column measured during all hydrocasts indicate active phytoplankton growth in the photic zone and respiration below. Oceanographic data measured below the thermocline indicate a homogenous and well mixed status of the water masses, which are believed to enter the Skagerrak from the south-western slope of the Norwegian Trench and are renewed every 100 days by a cyclonic current system (Rodhe, 1996). The cyclonic mixing, however, is probably reaching only water depths of 400-500 m and stagnant water is estimated below these depths (Rodhe, 1996). The decrease of

dissolved oxygen content below 560 m in sampling area N1 is probably due to this stagnant status (VCTD2-profile; Fig. 5.12).

The turbidity data indicating suspended matter in the water column exhibits three maxima in area N3, one in the surface water layer, second at about 120 mbsl and the third near the seafloor. However, the turbidity maximum at 120 m is missing in area N1 data (Fig. 5.12). Our sampling and further analytical strategy for water column sampling in the Skagerrak focussed on these maxima and near sea floor particles, which is a mix of in situ production and resuspended/transported material (Rodhe, 1996). The recorded CTD parameters during sampling and further subsampling details of Niskin water samples are given in the appendix (Tab. A12.2).

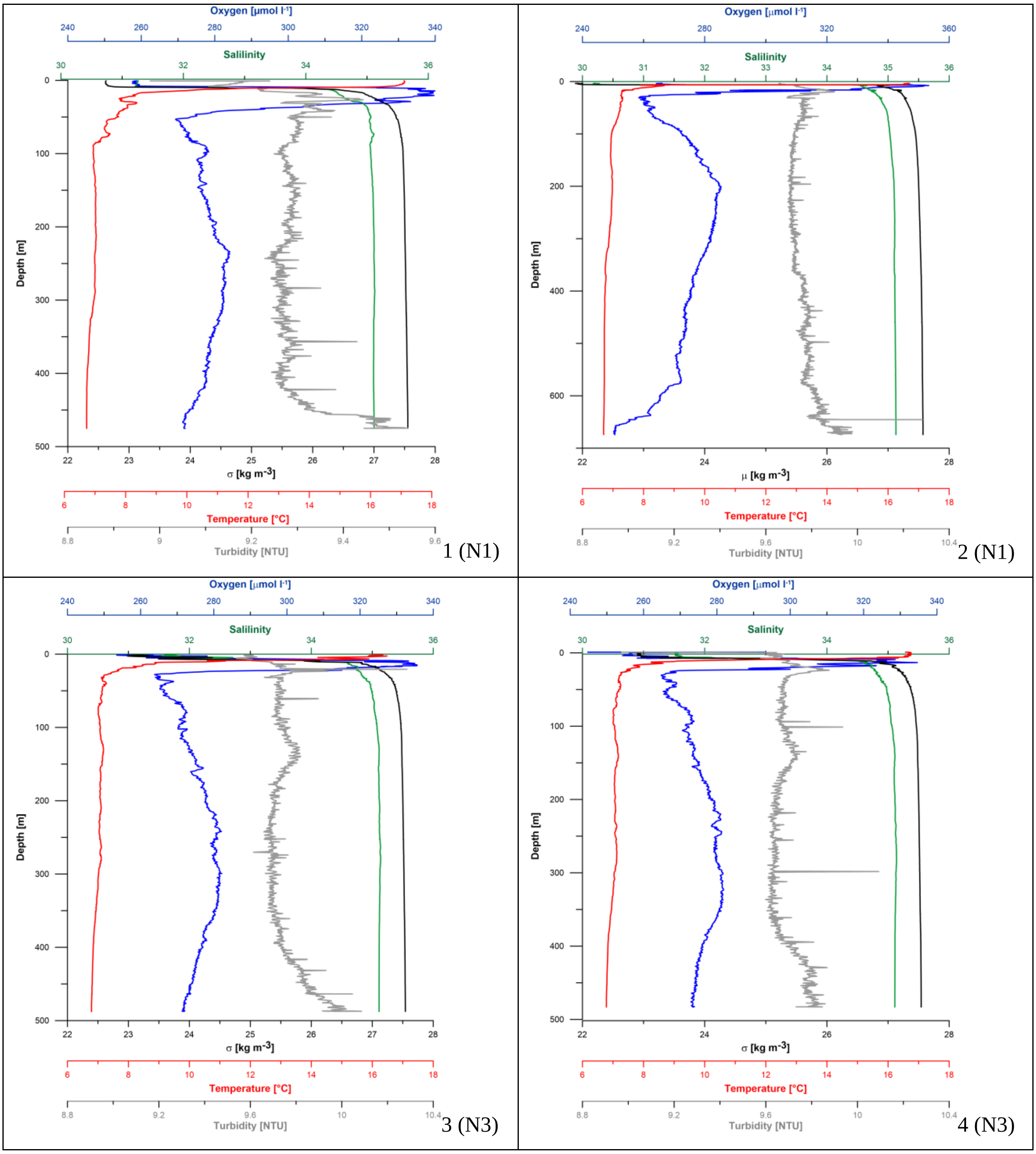


**Fig. 5.12** Raw CTD data recorded during 4 down-casts in the Skagerrak. VCTD 1-4 are ordered from upper left to lower right. The area index presented in Fig. 3.2 is given in brackets here.

### 5.2.4 Atmospheric Gas Measurements

(T. Weiss[1], M. Schmidt[1], C. Böttner[1])
[1]GEOMAR

Atmospheric $CO_2$ and $CH_4$ concentrations were monitored during the cruise using a cavity ring down spectrometer (Picarro G2301-f CRDS) and GEOMARs 'Atmospheric Intake System' (AIS). The Picarro/AIS system was installed in the wet laboratory (starboard, main deck) of RV Alkor and was connected to one air inlet placed on the “Back” deck of RV Alkor (Fig. 5.13). The air was pumped via an aluminium tubing into the Picarro analyzer. The atmospheric $CH_4$, $CO_2$, and water vapour concentrations were determined in real time at 2-3 Hz sampling rate. All data were logged on the Picarro PC in 1 hour-separated files. A time offset of 96 seconds between the air intake nozzle at the bow (“Back” deck at about 6 m above sea surface) and the actual gas measurement at the Picarro was determined and a calculated flow rate of 2.35 litre per minute considered, when correlating the gas data with navigation and weather data. Data merging of ship and Picarro data and subsequent statistical calculations will be conducted by the software package GEOMAR DATA WORKBENCH (software designed by T. Weiß).

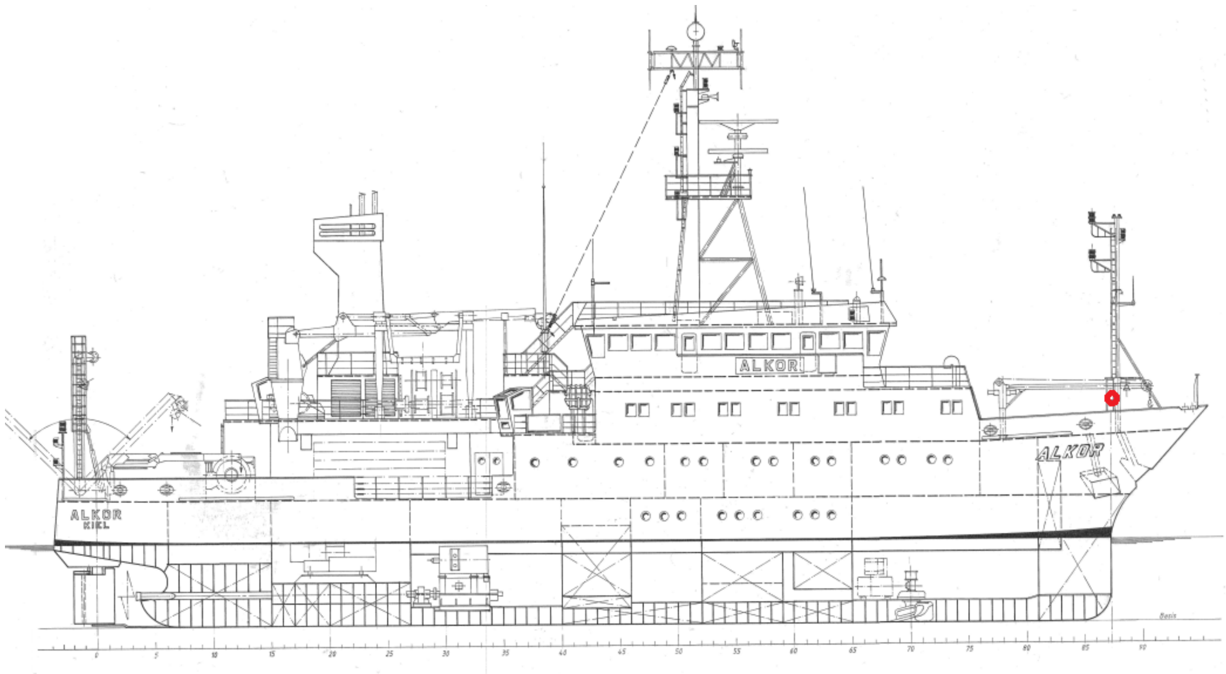


**Fig. 5.13** The inlet nozzle point on the “Back” deck of RV Alkor is marked on the sketch of the research vessel with a red dot.

## 6 Ship's Meteorological Station

(T. Weiss[1], M. Schmidt[1])

[1]GEOMAR

Weather data measured with onboard meteorological stations are needed in addition to the measured atmospheric methane and $CO_2$ data for calculating lateral distribution of sea-air gas flux. Therefore, the latitude, longitude, date, time, wind speed, water temperature etc. data logged by the DSHIP data system of RV Alkor will be used for further onshore data evaluation and spatial statistical calculations (https://dship.geomar.de/).

# 7 Station List AL561

## 7.1 Overall Station List

| Station No. | | Date | Gear | Time | Latitude | Longitude | Water Depth | Remarks |
|---|---|---|---|---|---|---|---|---|
| Alkor No. | Science No. | | | [UTC] | [N] | [E] | [m] | |
| AL561_1-1 | 1 | 03.08.2021 | SBP | 6:15 | 57° 27,052' | 011° 31,108' | 64 | profile start |
| AL561_1-1 | 1 | 03.08.2021 | SBP | 6:45 | 57° 27,145' | 011° 30,995' | 65 | profile end |
| AL561_2-1 | 2 | 03.08.2021 | MUC | 7:36 | 57° 27,027' | 011° 30,476' | 65 | in the water |
| AL561_2-1 | 2 | 03.08.2021 | MUC | 7:46 | 57° 27,025' | 011° 30,478' | 65 | on deck |
| AL561_3-1 | 3 | 03.08.2021 | GC | 11:19 | 57° 27,025' | 011° 30,480' | 65 | in the water |
| AL561_3-1 | 3 | 03.08.2021 | GC | 11:28 | 57° 27,021' | 011° 30,477' | 65 | on deck |
| AL561_4-1 | 4 | 03.08.2021 | SBP | 19:43 | 58° 10,753' | 009° 49,861' | 486 | profile start |
| AL561_4-1 | 4 | 04.08.2021 | SBP | 4:48 | 58° 10,676' | 009° 48,795' | 493 | profile end |
| AL561_5-1 | 5 | 04.08.2021 | BIGO | 8:41 | 58° 10,978' | 009° 47,237' | 503 | in the water |
| AL561_5-1 | 5 | 04.08.2021 | BIGO | 9:08 | 58° 10,969' | 009° 47,236' | 503 | deployed |
| AL561_5-1 | 5 | 06.08.2021 | BIGO | 6:03 | 58° 11,041' | 009° 46,972' | 496 | released |
| AL561_5-1 | 5 | 06.08.2021 | BIGO | 6:21 | 58° 11,045' | 009° 47,267' | 494 | recovered |
| AL561_6-1 | 6 | 04.08.2021 | VCTD | 10:03 | 58° 10,874' | 009° 47,628' | 500 | in the water |
| AL561_6-1 | 6 | 04.08.2021 | VCTD | 10:18 | 58° 10,881' | 009° 47,617' | 500 | on deck |
| AL561_6-2 | 6 | 04.08.2021 | VCTD | 10:28 | 58° 10,884' | 009° 47,611' | 500 | in the water |
| AL561_6-2 | 6 | 04.08.2021 | VCTD | 11:06 | 58° 10,885' | 009° 47,616' | 500 | on deck |
| AL561_7-1 | 7 | 04.08.2021 | MUC | 11:23 | 58° 10,884' | 009° 47,616' | 500 | in the water |
| AL561_7-1 | 7 | 04.08.2021 | MUC | 11:57 | 58° 10,880' | 009° 47,607' | 500 | on deck |
| AL561_8-1 | 8 | 04.08.2021 | GC | 13:18 | 58° 10,882' | 009° 47,612' | 500 | in the water |
| AL561_8-1 | 8 | 04.08.2021 | GC | 13:44 | 58° 10,872' | 009° 47,614' | 500 | on deck |
| AL561_8-2 | 8 | 04.08.2021 | GC | 14:49 | 58° 10,882' | 009° 47,622' | 500 | in the water |
| AL561_8-2 | 8 | 04.08.2021 | GC | 15:16 | 58° 10,871' | 009° 47,593' | 500 | on deck |
| AL561_9-1 | 9 | 04.08.2021 | SBP | 19:16 | 58° 38,564' | 010° 05,426' | 450 | profile start |
| AL561_9-1 | 9 | 05.08.2021 | SBP | 4:48 | 58° 45,353' | 010° 10,282' | 240 | profile end |
| AL561_10-2 | 10 | 05.08.2021 | GC | 6:27 | 58° 44,878' | 010° 13,449' | 214 | in the water |
| AL561_10-2 | 10 | 05.08.2021 | GC | 6:38 | 58° 44,874' | 010° 13,454' | 215 | on deck |
| AL561_10-1 | 10 | 05.08.2021 | GC | 6:02 | 58° 44,871' | 010° 13,448' | 215 | in the water |
| AL561_10-1 | 10 | 05.08.2021 | GC | 6:24 | 58° 44,883' | 010° 13,456' | 215 | on deck |
| AL561_11-2 | 11 | 05.08.2021 | MUC | 7:30 | 58° 44,880' | 010° 13,442' | 215 | in the water |
| AL561_11-2 | 11 | 05.08.2021 | MUC | 7:57 | 58° 44,876' | 010° 13,429' | 213 | on deck |
| AL561_11-1 | 11 | 05.08.2021 | MUC | 6:58 | 58° 44,873' | 010° 13,445' | 215 | in the water |
| AL561_11-1 | 11 | 05.08.2021 | MUC | 7:21 | 58° 44,874' | 010° 13,443' | 213 | on deck |
| AL561_12-4 | 12 | 05.08.2021 | GC | 11:30 | 58° 44,878' | 010° 13,450' | 215 | in the water |
| AL561_12-4 | 12 | 05.08.2021 | GC | 11:44 | 58° 44,881' | 010° 13,446' | 215 | on deck |
| AL561_12-3 | 12 | 05.08.2021 | GC | 11:07 | 58° 44,878' | 010° 13,448' | 215 | in the water |
| AL561_12-3 | 12 | 05.08.2021 | GC | 11:18 | 58° 44,880' | 010° 13,456' | 215 | on deck |
| AL561_12-2 | 12 | 05.08.2021 | GC | 10:29 | 58° 44,879' | 010° 13,448' | 215 | in the water |

| | | | | | | | | |
|---|---|---|---|---|---|---|---|---|
| AL561_12-2 | 12 | 05.08.2021 | GC | 10:42 | 58° 44,881' | 010° 13,445' | 215 | on deck |
| AL561_12-1 | 12 | 05.08.2021 | GC | 8:57 | 58° 44,873' | 010° 13,434' | 215 | in the water |
| AL561_12-1 | 12 | 05.08.2021 | GC | 9:15 | 58° 44,873' | 010° 13,420' | 215 | on deck |
| AL561_13-1 | 13 | 05.08.2021 | VCTD | 15:52 | 58° 18,789' | 009° 34,339' | 379 | in the water |
| AL561_13-1 | 13 | 05.08.2021 | VCTD | 17:20 | 58° 18,782' | 009° 34,362' | 694 | on deck |
| AL561_14-1 | 14 | 05.08.2021 | SBP | 19:19 | 58° 12,573' | 009° 00,446' | 423 | profile start |
| AL561_14-1 | 14 | 06.08.2021 | SBP | 3:24 | 57° 57,214' | 009° 17,664' | 300 | profile end |
| AL561_15-1 | 15 | 06.08.2021 | MUC | 9:07 | 58° 10,905' | 009° 47,577' | 492 | in the water |
| AL561_15-1 | 15 | 06.08.2021 | MUC | 9:33 | 58° 10,893' | 009° 47,638' | 492 | on deck |
| AL561_16-1 | 16 | 06.08.2021 | GC | 11:05 | 58° 10,892' | 009° 47,594' | 492 | in the water |
| AL561_16-1 | 16 | 06.08.2021 | GC | 11:31 | 58° 10,891' | 009° 47,569' | 492 | on deck |
| AL561_17-1 | 17 | 06.08.2021 | BIGO | 15:31 | 58° 18,783' | 009° 34,367' | 676 | deployed |
| AL561_17-1 | 17 | 08.08.2021 | BIGO | 6:01 | 58° 18,778' | 009° 34,184' | 677 | released |
| AL561_17-1 | 17 | 08.08.2021 | BIGO | 6:21 | 58° 18,774' | 009° 34,224' | 677 | recovered |
| AL561_18-1 | 18 | 06.08.2021 | SBP | 20:30 | 57° 52,116' | 008° 11,017' | 517 | profile start |
| AL561_18-1 | 18 | 07.08.2021 | SBP | 5:06 | 57° 52,942' | 008° 15,089' | 500 | profile end |
| AL561_19-2 | 19 | 07.08.2021 | MUC | 14:13 | 57° 45,197' | 008° 17,174' | 434 | in the water |
| AL561_19-2 | 19 | 07.08.2021 | MUC | 14:40 | 57° 45,186' | 008° 17,170' | 434 | on deck |
| AL561_19-1 | 19 | 07.08.2021 | MUC | 13:41 | 57° 45,187' | 008° 17,175' | 434 | in the water |
| AL561_19-1 | 19 | 07.08.2021 | MUC | 14:12 | 57° 45,199' | 008° 17,168' | 434 | on deck |
| AL561_20-1 | 20 | 07.08.2021 | MUC | 16:05 | 57° 38,093' | 008° 23,972' | 186 | in the water |
| AL561_20-1 | 20 | 07.08.2021 | MUC | 16:24 | 57° 38,082' | 008° 23,997' | 184 | on deck |
| AL561_21-1 | 21 | 07.08.2021 | SBP | 21:19 | 58° 05,574' | 009° 32,105' | 485 | profile start |
| AL561_21-1 | 21 | 08.08.2021 | SBP | 5:18 | 58° 15,108' | 009° 24,816' | 681 | profile end |
| AL561_21-1 | 21 | 07.08.2021 | SBP | 19:58 | 57° 57,430' | 009° 15,261' | 360 | profile start |
| AL561_21-1 | 21 | 07.08.2021 | SBP | 20:38 | 58° 00,585' | 009° 21,533' | 447 | profile end |
| AL561_22-1 | 22 | 08.08.2021 | MUC | 8:25 | 58° 18,777' | 009° 34,327' | 677 | in the water |
| AL561_22-1 | 22 | 08.08.2021 | MUC | 9:21 | 58° 18,723' | 009° 34,089' | 677 | on deck |
| AL561_23-1 | 23 | 08.08.2021 | GC | 11:33 | 58° 18,787' | 009° 34,334' | 677 | in the water |
| AL561_23-1 | 23 | 08.08.2021 | GC | 13:00 | 58° 16,785' | 009° 32,432' | 691 | on deck |
| AL561_24-1 | 24 | 08.08.2021 | BIGO | 16:07 | 57° 59,233' | 009° 14,305' | 490 | in the water |
| AL561_24-1 | 24 | 08.08.2021 | BIGO | 16:28 | 57° 59,229' | 009° 14,298' | 490 | released |
| AL561_24-1 | 24 | 10.08.2021 | BIGO | 6:03 | 57° 59,342' | 009° 14,431' | 490 | released |
| AL561_24-1 | 24 | 10.08.2021 | BIGO | 6:11 | 57° 59,322' | 009° 14,432' | 490 | at surface |
| AL561_24-1 | 24 | 10.08.2021 | BIGO | 6:32 | 57° 59,287' | 009° 14,664' | 491 | on deck |
| AL561_25-1 | 25 | 09.08.2021 | VCTD | 6:02 | 57° 59,305' | 009° 14,291' | 490 | in the water |
| AL561_25-1 | 25 | 09.08.2021 | VCTD | 7:05 | 57° 59,298' | 009° 14,314' | 490 | on deck |
| AL561_26-1 | 26 | 09.08.2021 | VCTD | 8:06 | 57° 59,279' | 009° 14,296' | 490 | in the water |
| AL561_26-1 | 26 | 09.08.2021 | VCTD | 9:01 | 57° 59,281' | 009° 14,286' | 490 | on deck |
| AL561_27-1 | 27 | 09.08.2021 | MUC | 10:18 | 57° 59,281' | 009° 14,295' | 490 | in the water |
| AL561_27-1 | 27 | 09.08.2021 | MUC | 10:44 | 57° 59,290' | 009° 14,315' | 490 | on deck |

| | | | | | | | | |
|---|---|---|---|---|---|---|---|---|
| AL561_28-1 | 28 | 09.08.2021 | GC | 11:35 | 57° 59,273' | 009° 14,361' | 490 | in the water |
| AL561_28-1 | 28 | 09.08.2021 | GC | 11:55 | 57° 59,263' | 009° 14,316' | 488 | on deck |
| AL561_29-1 | 29 | 09.08.2021 | SBP | 12:47 | 57° 58,530' | 009° 13,315' | 478 | profile start |
| AL561_29-1 | 29 | 09.08.2021 | SBP | 13:36 | 58° 01,743' | 009° 19,650' | 489 | profile end |
| AL561_30-1 | 30 | 09.08.2021 | SBP | 14:42 | 58° 05,115' | 009° 04,514' | 612 | profile start |
| AL561_30-1 | 30 | 09.08.2021 | SBP | 16:29 | 57° 57,262' | 009° 17,357' | 308 | profile end |
| AL561_31-1 | 31 | 10.08.2021 | MUC | 10:04 | 58° 04,357' | 009° 05,756' | 604 | in the water |
| AL561_31-1 | 31 | 10.08.2021 | MUC | 10:38 | 58° 04,352' | 009° 05,739' | 604 | on deck |
| AL561_32-1 | 32 | 10.08.2021 | GC | 12:09 | 58° 04,344' | 009° 05,765' | 604 | in the water |
| AL561_32-1 | 32 | 10.08.2021 | GC | 12:32 | 58° 04,355' | 009° 05,740' | 604 | on deck |
| AL561_33-1 | 33 | 10.08.2021 | SBP | 14:28 | 58° 12,877' | 009° 19,188' | 668 | profile start |
| AL561_33-1 | 33 | 10.08.2021 | SBP | 16:33 | 58° 20,227' | 009° 38,058' | 662 | profile end |
| AL561_34-1 | 34 | 11.08.2021 | GC | 6:02 | 57° 27,022' | 011° 30,491' | 67 | in the water |
| AL561_34-1 | 34 | 11.08.2021 | GC | 6:10 | 57° 27,018' | 011° 30,495' | 67 | on deck |

# 8 Data and Sample Storage and Availability

Physical samples taken during the expedition are stored at GEOMAR repositories and can be accessed on request. Local storage of sediment cores is provided by the GEOMAR lithothek, core and rock repository https://www.geomar.de/en/centre/central-facilities/tlz/core-rock-repository/.

Acquired hydroacoustic, video, and image raw data will be archived in the IT storage infrastructure at GEOMAR and is available on request. Meta data of the cruise can be found here:
https://portal.geomar.de/metadata/leg/show/359126.
https://www.geomar.de/forschen/expeditionen/detailansicht/exp/359692
All navigation, weather, echosounder, and surface water data recorded during AL561 is available for download at http://dship.geomar.de/
Evaluated data sets will be available through data repositories OSIS (https://portal.geomar.de/) and finally through Pangea (https://pangaea.de/). For further details see table 8.1.

**Table 8.1** Overview of data availability and responsibility.

| Type | Database | Available Date | Free Access Date | Contact E-Mail |
|---|---|---|---|---|
| VCTD data | OSIS/Pangaea | 01/2022 | 01/2024 | mschmidt@geomar.de |
| BIGO data | OSIS/Pangaea | 06/2022 | 01/2024 | ssommer@geomar.de |
| Porewater chemistry | OSIS/Pangaea | 06/2022 | 01/2024 | adale@geomar.de tspiegel@geomar.de |
| Sediment geochemistry | OSIS/Pangaea | 12/2022 | 01/2024 | nlenz@geomar.de adale@geomar.de |
| Hydroacoustic data | OSIS/Pangaea | 06/2022 | 01/2024 | christoph.boettner@ifg.uni-kiel.de |
| Picarro data | OSIS/Pangaea | 01/2022 | 01/2024 | tweiss@geomar.de |

## 9 Acknowledgements

This research cruise was approved by the "Gutachterpanel Forschungsschiffe" of the German Research Foundation under license no. GPF 21-2_028.

We highly acknowledge the financial support from BMBF, which was granted to GEOMAR under ID 03F0874B to conduct this research cruise and the subsequent experiments and analyses.

We acknowledge the professional onboard support of captain Tino Kaufmann and his crew.

## 10 References

Bakker, J.F., Helder, W., 1993. Skagerrak (northeastern North Sea) oxygen microprofiles and porewater chemistry in sediments. Marine Geology 111, 299-321.

Dale, A.W., Regnier, P., Knab, N.J., Jørgensen, B.B. and Van Cappellen, P., 2008. Anaerobic oxidation of methane (AOM) in marine sediments from the Skagerrak (Denmark): II. Reaction-transport modelling. Geochim. Cosmochim. Acta 72, 2880-2894.

Dando, P.R., Southward, A.J., Southward, E.C., Lamont, P., Harvey, R., 2008. Interactions between sediment chemistry and frenulate pogonophores (Annelida) in the north-east Atlantic. Deep-Sea Research I 55, 966-996.

de Haas, H., Boer, W., van Weering, T.C.E, 1997. Recent sediment and organic carbon burial in a shelf sea; the North Sea. Marine Geology 144, 131-146

de Haas, H., van Weering, T.C.E., 1997. Recent sediment accumulation, organic carbon burial and transport in the northeastern North Sea. Marine Geology 136, 173-187.

de Haas, H., van Weering, T.C.E., de Stigter, H., 2002. Organic carbon in shelf seas: sinks or sources, processes and products. Continental Shelf Research 22, 691-717.

Devol A. H. and Christensen J. P., 1993. Benthic fluxes and nitrogen cycling in sediments of the continental margin of the eastern North Pacific. J. Mar. Res. 51, 345–372.

Dickson, A.G., Sabine, C.L., Christian, J.R. (Eds), 2007. Guide to best practices for ocean $CO_2$ measurements. PICES Special Publication 3, 191 pp.

Diesing, M., Thorsnes, T., and Bjarnadóttir, L. R., 2021. Organic carbon densities and accumulation rates in surface sediments of the North Sea and Skagerrak. Biogeosciences 18, 2139-2160.

European Atlas of the Seas, 2021. https://ec.europa.eu/maritimeaffairs/atlas/maritime_atlas

Flügel, H.J., Langhof, I., 1982. Pogonophora in the Skagerrak. Sarsia 67, 211-212.

Hall, P.O.J., Hulth, S., Hulthe, G., Landén, A., Tengberg, A., 1996. Benthic nutrient fluxes on a basin-wide scale in the Skagerrak (North-Eastern North Sea). Journal of Sea Research, 35, 123-137.

Hedges, J.I., Baldock, J.A., Gélinas, Y., Lee, C., Peterson, M.L., Wakeham, S.G., 2002. The biochemical and elemental compositions of marine plankton: a NMR perspective. Marine Chemistry 78, 47–63.

Hempel, P., Spiess, V., Schreiber, R., 1994. Expulsion of shallow gas in the Skagerrak—evidence from sub-bottom profiling, seismic, hydroacoustical and geochemical data. Estuarine, Coastal and Shelf Science, 38(6), 583-601.

Irion, G., Zöllmer, V., 1999. Clay mineral associations in fine-grained surface sediments of the North Sea. J. Sea Research 41, 119–128.

Kirkegaard, J.B., 1958. Records of the group pogonophara in the Skagerrak. Nature 181, 1086-1087.

Knab, N. J., Cragg, B. A., Borowski C., Parkes J. R., Pancost, R., and Jørgensen B. B., 2008. Anaerobic oxidation of methane (AOM) in marine sediments from the Skagerrak (Denmark): I. Geochemical and microbiological analyses. Geochim. Cosmochim. Acta 72, 2868–2879.

Kuijpers, A., Dennegard, B., Albinsson, Y., Jensen, A., 1993. Sediment transport pathways in the Skagerrak and Kattegat as indicated by sediment Chernobyl radioactivity and heavy-metal concentrations. Mar. Geol. 111, 231-244.

Laier, T., Jensen, J. B., 2007. Shallow gas depth-contour map of the Skagerrak-western Baltic Sea region. Geo-Marine Letters, 27(2-4), 127-141.

Longva, O., Olsen, H. A., Piper, D. J., Rise, L., Thorsnes, T., 2008. Late glacial fans in the eastern Skagerrak; depositional environment interpreted from swath bathymetry and seismostratigraphy. Marine Geology, 251(1-2), 110-123.

Rise, L., Sættem, J., Fanavoll, S., Thorsnes, T., Ottesen, D., Bøe, R., 1999. Sea-bed pockmarks related to fluid migration from Mesozoic bedrock strata in the Skagerrak offshore Norway. Marine and Petroleum Geology, 16(7), 619-631.

Rodhe J., 1996. On the dynamics of the large-scale circulation of the Skagerrak. Journal of Sea Research 35 (1-3), 9-21.

Ruttenberg K. C. and Berner R. A., 1993. Authigenic apatite formation and burial in sediments from non-upwelling, continental margin environments. Geochim. Cosmochim. Acta 57, 991–1007.

Smith, W.H., Sandwell, D.T., 1997. Global Sea Floor Topography from Satellite Altimetry and Ship Depth Soundings. Science 277, 1956-1962.

Sommer, S., Linke, P., Pfannkuche, P., Schleicher, T., Schneider v. Deimling, J., Reitz, A., Haeckel, M., Flögel, S., Hensen, C., 2009. Seabed methane emissions and the habitat of frenulate tubeworms on the Captain Arutyunov mud volcano (Gulf of Cadiz). Marine Ecology Progress Series 382, 69-86.

Ståhl, H., Tengberg, A., Brunnegård, J., Bjørnbom, E., Forbes, T.L., Josefson, A.B., Kaberi, H.G., Karle Hassellöv, I.M., Olsgard, F., Roos, P., Hall, P.O.J., 2004. Factors influencing organic carbon recycling and burial in Skagerrak sediments. Journal of Marine Research 62, 867-907.

Wunderlich, J., Müller, S., 2003. High-resolution sub-bottom profiling using parametric acoustics. International Ocean Systems 7, 6-11.

## 11 Abbreviations

| | |
|---|---|
| AIS | Atmospheric Intake System |
| AOM | Anaerobe Oxidation of Methane |
| APOC | Anthropogenic impacts on Particulate Organic Carbon cycling in the North Sea |
| BIGO | Biogeochemical Observatory |
| $C_{org}$ deg. | Organic Carbon degradation |
| GC | Gravity Corer |
| GCOAST | Geesthacht Coupled cOAstal model SysTem |

| | |
|---|---|
| mbsl | meter below sea level |
| MUC | Multi-Corer |
| POC | Particulate Organic Carbon |
| SPM | Suspended Particulate Matter |
| VCTD | Video controlled Conductivity/Temperature/Depth sensor device |

# 12 Appendices

## 12.1 Selected Tables

**Table A12.1** Specific times of water sampling during all lander deployments conducted during cruise AL561 (BIGO-II-1, BIGO-II-2, BIGO-II-3). CH1, CH2, and BW denotes the sampling in Chamber 1, Chamber 2 and Bottom water respectively. The number added indicates the number of the glass syringe taken. The water sampling using the glass tubes is denoted in a similar way and indicated by the extension 'Tube'. Start refers to the actual activation of the lander onboard just prior to its deployment. The abbreviation Synchro refers to the time when both benthic chambers were driven into the sediment and the actual flux measurement in both chambers is started synchronously. Slide down indicates the time when the shutter was driven underneath the benthic chamber so that upon lander retrieval the sediment is retained.

| | | | | | | | | | | | |
|---|---|---|---|---|---|---|---|---|---|---|---|
| **AL561 2021** | | | | | | | | | | | |
| **Skagerrak** | | | | | | | | | | | |
| **BIGO-II-1** | | | | **BIGO-II-2** | | | | **BIGO-II-2** | | | |
| **Start** | 04.08.21 08:35 | | | **Start** | 06.08.21 14:44 | | | **Start** | 08.08.21 15:57 | | |
| **Synchro** | 04.08.21 12:06 | | | **Synchro** | 06.08.21 20:22 | | | **Synchro** | 08.08.21 21:35 | | |
| | | | | | | | | | | | |
| **CH1_1** | 04.08.21 12:21 | **CH1_Tube_1** | 04.08.21 12:59 | **CH1_1** | 06.08.21 20:37 | **CH1_Tube_1** | 06.08.21 21:17 | **CH1_1** | 08.08.21 21:50 | **CH1_Tube_1** | 08.08.21 22:31 |
| **CH1_2** | 04.08.21 17:25 | **CH1_Tube_2** | 04.08.21 17:54 | **CH1_2** | 07.08.21 00:41 | **CH1_Tube_2** | 07.08.21 01:12 | **CH1_2** | 09.08.21 01:54 | **CH1_Tube_2** | 09.08.21 02:27 |
| **CH1_3** | 04.08.21 22:29 | **CH1_Tube_3** | 04.08.21 22:51 | **CH1_3** | 07.08.21 04:45 | **CH1_Tube_3** | 07.08.21 05:09 | **CH1_3** | 09.08.21 05:58 | **CH1_Tube_3** | 09.08.21 06:24 |
| **CH1_4** | 05.08.21 03:33 | **CH1_Tube_4** | 05.08.21 03:48 | **CH1_4** | 07.08.21 08:49 | **CH1_Tube_4** | 07.08.21 09:05 | **CH1_4** | 09.08.21 10:02 | **CH1_Tube_4** | 09.08.21 10:20 |
| **CH1_5** | 05.08.21 08:38 | **CH1_Tube_5** | 05.08.21 08:42 | **CH1_5** | 07.08.21 12:54 | **CH1_Tube_5** | 07.08.21 13:01 | **CH1_5** | 09.08.21 14:07 | **CH1_Tube_5** | 09.08.21 14:16 |
| **CH1_6** | 05.08.21 13:42 | **CH1_Tube_6** | 05.08.21 13:39 | **CH1_6** | 07.08.21 16:58 | **CH1_Tube_6** | 07.08.21 16:57 | **CH1_6** | 09.08.21 18:11 | **CH1_Tube_6** | 09.08.21 18:13 |
| **CH1_7** | 05.08.21 18:46 | **CH1_Tube_7** | 05.08.21 18:35 | **CH1_7** | 07.08.21 21:02 | **CH1_Tube_7** | 07.08.21 20:53 | **CH1_7** | 09.08.21 22:15 | **CH1_Tube_7** | 09.08.21 22:08 |
| **CH1_8** | 05.08.21 23:51 | **CH1_Tube_8** | 05.08.21 23:31 | **CH1_8** | 08.08.21 01:07 | **CH1_Tube_8** | 08.08.21 00:49 | **CH1_8** | 10.08.21 02:20 | **CH1_Tube_8** | 10.08.21 02:04 |
| **CH2_1** | 04.08.21 12:21 | **CH2_Tube_1** | 04.08.21 12:59 | **CH2_1** | 06.08.21 20:37 | **CH2_Tube_1** | 06.08.21 21:17 | **CH2_1** | 08.08.21 21:50 | **CH2_Tube_1** | 08.08.21 22:31 |
| **CH2_2** | 04.08.21 17:25 | **CH2_Tube_2** | 04.08.21 17:54 | **CH2_2** | | **CH2_Tube_2** | 07.08.21 01:12 | **CH2_2** | 09.08.21 01:54 | **CH2_Tube_2** | 09.08.21 02:27 |
| **CH2_3** | 04.08.21 22:29 | **CH2_Tube_3** | 04.08.21 22:51 | **CH2_3** | 07.08.21 04:45 | **CH2_Tube_3** | 07.08.21 05:09 | **CH2_3** | 09.08.21 05:58 | **CH2_Tube_3** | 09.08.21 06:24 |
| **CH2_4** | 05.08.21 03:33 | **CH2_Tube_4** | 05.08.21 03:48 | **CH2_4** | 07.08.21 08:49 | **CH2_Tube_4** | 07.08.21 09:05 | **CH2_4** | 09.08.21 10:02 | **CH2_Tube_4** | 09.08.21 10:20 |
| **CH2_5** | | **CH2_Tube_5** | 05.08.21 08:42 | **CH2_5** | 07.08.21 12:54 | **CH2_Tube_5** | 07.08.21 13:01 | **CH2_5** | 09.08.21 14:07 | **CH2_Tube_5** | 09.08.21 14:16 |
| **CH2_6** | 05.08.21 13:42 | **CH2_Tube_6** | 05.08.21 13:39 | **CH2_6** | 07.07.21 16:58 | **CH2_Tube_6** | 07.08.21 16:57 | **CH2_6** | 09.08.21 18:11 | **CH2_Tube_6** | 09.08.21 18:13 |
| **CH2_7** | 05.08.21 18:46 | **CH2_Tube_7** | 05.08.21 18:35 | **CH2_7** | 07.08.21 21:02 | **CH2_Tube_7** | 07.08.21 20:53 | **CH2_7** | 09.08.21 22:15 | **CH2_Tube_7** | 09.08.21 22:08 |
| **CH2_8** | | **CH2_Tube_8** | 05.08.21 23:31 | **CH2_8** | 08.08.21 01:07 | **CH2_Tube_8** | 08.08.21 00:49 | **CH2_8** | 10.08.21 02:20 | **CH2_Tube_8** | 10.08.21 02:04 |
| **BW_1** | 04.08.21 12:21 | **BW_Tube_1** | 04.08.21 12:59 | **BW_1** | 06.08.21 20:37 | **BW_Tube_1** | 06.08.21 21:17 | **BW_1** | 08.08.21 21:50 | **BW_Tube_1** | 08.08.21 22:31 |
| **BW_2** | 04.08.21 17:25 | **BW_Tube_2** | 04.08.21 17:54 | **BW_2** | 07.08.21 00:41 | **BW_Tube_2** | 07.08.21 01:12 | **BW_2** | 09.08.21 01:54 | **BW_Tube_2** | 09.08.21 02:27 |
| **BW_3** | 04.08.21 22:29 | **BW_Tube_3** | 04.08.21 22:51 | **BW_3** | 07.08.21 04:45 | **BW_Tube_3** | 07.08.21 05:09 | **BW_3** | 09.08.21 05:58 | **BW_Tube_3** | 09.08.21 06:24 |
| **BW_4** | 05.08.21 03:33 | **BW_Tube_4** | 05.08.21 03:48 | **BW_4** | 07.08.21 08:49 | **BW_Tube_4** | 07.08.21 09:05 | **BW_4** | 09.08.21 10:02 | **BW_Tube_4** | 09.08.21 10:20 |
| **BW_5** | 05.08.21 08:38 | **BW_Tube_5** | 05.08.21 08:42 | **BW_5** | 07.08.21 12:54 | **BW_Tube_5** | 07.08.21 13:01 | **BW_5** | 09.08.21 14:07 | **BW_Tube_5** | 09.08.21 14:16 |
| **BW_6** | 05.08.21 13:42 | **BW_Tube_6** | 05.08.21 13:39 | **BW_6** | 07.08.21 16:58 | **BW_Tube_6** | 07.08.21 16:57 | **BW_6** | 09.08.21 18:11 | **BW_Tube_6** | 09.08.21 18:13 |
| **BW_7** | 05.08.21 18:46 | **BW_Tube_7** | 05.08.21 18:35 | **BW_7** | 07.08.21 21:02 | **BW_Tube_7** | 07.08.21 20:53 | **BW_7** | 09.08.21 22:15 | **BW_Tube_7** | 09.08.21 22:08 |
| **BW_8** | 05.08.21 23:51 | **BW_Tube_8** | 05.08.21 23:31 | **BW_8** | 08.08.21 01:07 | **BW_Tube_8** | 08.08.21 00:49 | **BW_8** | 10.08.21 02:20 | **BW_Tube_8** | 10.08.21 02:04 |
| **Slide down** | 06.08.21 00:51 | **Slide down** | 06.08.21 00:50 | **Slide down** | 08.08.21 02:10 | **Slide down** | 08.08.21 02:13 | **Slide down** | 10.08.21 03:25 | **Slide down** | 10.08.21 03:29 |

**Table A12.2** Summary of bottle files shows selected CTD parameters for sampled Niskin bottles. Subsampling of Niskin water samplers for additional parameters are listed under remarks (F – filtration of SPM; N – nutrient analyses; Nd – Nd-isotope analyses; S – laboratory seawater standard).

| Niskin No. | Time | Date | $O_2$ /mmol kg-1 | Depth /m | Temp. /°C | Salinity | Latitude /°N | Longitude /°E | Fluorescense /a.u. | Remarks |
|---|---|---|---|---|---|---|---|---|---|---|
| VCTD1 | | | | | | | | | | |
| 2 | 10:52:34 | 04.08.2021 | 295,5 | 475,0 | 6,728 | 35,114 | 58,181 | 9,7935 | 0,45 | Nd, N |
| 3 | 10:52:37 | 04.08.2021 | 295,5 | 475,1 | 6,728 | 35,114 | 58,181 | 9,7935 | 0,44 | |
| 4 | 10:57:05 | 04.08.2021 | 295,0 | 357,1 | 6,807 | 35,109 | 58,181 | 9,7936 | 0,43 | N |
| 5 | 10:57:06 | 04.08.2021 | 295,0 | 356,4 | 6,807 | 35,109 | 58,181 | 9,7936 | 0,42 | |
| 6 | 11:03:21 | 04.08.2021 | 293,5 | 153,4 | 7,025 | 35,099 | 58,181 | 9,7935 | 0,43 | |
| 7 | 11:03:22 | 04.08.2021 | 293,5 | 152,8 | 7,022 | 35,098 | 58,181 | 9,7935 | 0,43 | N |
| 8 | 11:07:33 | 04.08.2021 | 285,1 | 31,4 | 8,345 | 34,944 | 58,181 | 9,7936 | 4,89 | N |
| 9 | 11:07:34 | 04.08.2021 | 285,1 | 30,9 | 8,353 | 34,934 | 58,181 | 9,7936 | 4,81 | |
| 10 | 11:08:17 | 04.08.2021 | 281,7 | 15,8 | 9,035 | 34,502 | 58,181 | 9,7936 | 2,11 | N |
| 11 | 11:08:18 | 04.08.2021 | 280,8 | 15,5 | 9,173 | 34,492 | 58,181 | 9,7936 | 2,09 | |
| 12 | 11:08:46 | 04.08.2021 | 244,5 | 6,0 | 16,950 | 31,234 | 58,181 | 9,7936 | 0,92 | Nd |
| VCTD2 | | | | | | | | | | |
| 2 | 16:41:49 | 05.08.2021 | 295,7 | 670,0 | 6,692 | 35,129 | 58,313 | 9,57268 | 0,46 | Nd, N |
| 3 | 16:41:51 | 05.08.2021 | 295,7 | 670,0 | 6,692 | 35,129 | 58,313 | 9,57268 | 0,46 | F, N |
| 4 | 16:51:28 | 05.08.2021 | 295,6 | 632,4 | 6,705 | 35,128 | 58,313 | 9,57278 | 0,45 | Nd, N |
| 5 | 16:58:21 | 05.08.2021 | 295,5 | 420,7 | 6,732 | 35,112 | 58,313 | 9,57288 | 0,44 | F, N |
| 6 | 17:05:29 | 05.08.2021 | 293,9 | 200,9 | 6,976 | 35,098 | 58,313 | 9,5729 | 0,44 | Nd |
| 7 | 17:05:57 | 05.08.2021 | 293,9 | 186,7 | 6,973 | 35,093 | 58,313 | 9,5729 | 0,43 | F, N |
| 8 | 17:16:55 | 05.08.2021 | 292,0 | 31,2 | 7,317 | 34,871 | 58,313 | 9,57278 | 2,10 | F, N |
| 9 | 17:16:57 | 05.08.2021 | 292,0 | 31,2 | 7,317 | 34,871 | 58,313 | 9,57278 | 2,09 | F, N |
| 10 | 17:18:29 | 05.08.2021 | 290,4 | 16,1 | 7,624 | 34,697 | 58,313 | 9,57278 | 4,30 | F, N |
| 11 | 17:18:31 | 05.08.2021 | 290,4 | 16,1 | 7,624 | 34,698 | 58,313 | 9,57278 | 4,30 | F, N |
| 12 | 17:19:35 | 05.08.2021 | 274,4 | 6,1 | 10,543 | 33,534 | 58,313 | 9,57278 | 1,57 | Nd |
| VCTD3 | | | | | | | | | | |
| 2 | 06:44:23 | 09.08.2021 | 295,1 | 483,3 | 6,789 | 35,112 | 57,988 | 9,23852 | 0,44 | Nd |
| 3 | 06:44:24 | 09.08.2021 | 295,1 | 483,3 | 6,789 | 35,112 | 57,988 | 9,23852 | 0,43 | Nd |
| 4 | 06:56:52 | 09.08.2021 | 293,2 | 252,1 | 7,062 | 35,122 | 57,988 | 9,23852 | 0,42 | F |
| 5 | 06:56:54 | 09.08.2021 | 293,2 | 252,2 | 7,061 | 35,123 | 57,988 | 9,23852 | 0,42 | F |
| 6 | 07:01:58 | 09.08.2021 | 293,3 | 102,1 | 7,066 | 35,078 | 57,988 | 9,23838 | 0,43 | Nd, F |
| 7 | 07:02:00 | 09.08.2021 | 293,3 | 102,3 | 7,067 | 35,079 | 57,988 | 9,23838 | 0,45 | Nd, F |
| 8 | 07:04:39 | 09.08.2021 | 293,2 | 31,9 | 7,151 | 34,852 | 57,988 | 9,23846 | 1,53 | F |
| 9 | 07:05:27 | 09.08.2021 | 290,1 | 21,9 | 7,645 | 34,746 | 57,988 | 9,23852 | 5,50 | S |
| 10 | 07:05:28 | 09.08.2021 | 290,1 | 22,1 | 7,652 | 34,753 | 57,988 | 9,23852 | 5,71 | S |
| 11 | 07:05:30 | 09.08.2021 | 289,9 | 22,2 | 7,670 | 34,764 | 57,988 | 9,23852 | 5,76 | S |
| 12 | 07:05:59 | 09.08.2021 | 285,8 | 16,8 | 8,309 | 34,728 | 57,988 | 9,23856 | 5,37 | F |
| VCTD4 | | | | | | | | | | |
| 2 | 08:47:50 | 09.08.2021 | 295,1 | 483,0 | 6,782 | 35,110 | 57,988 | 9,23808 | 0,43 | S |
| 3 | 08:47:51 | 09.08.2021 | 295,1 | 482,9 | 6,783 | 35,110 | 57,988 | 9,23808 | 0,43 | S |
| 4 | 08:47:52 | 09.08.2021 | 295,1 | 482,8 | 6,782 | 35,110 | 57,988 | 9,23808 | 0,43 | S |
| 5 | 08:47:53 | 09.08.2021 | 295,1 | 482,8 | 6,782 | 35,110 | 57,988 | 9,23808 | 0,42 | S |
| 6 | 09:03:24 | 09.08.2021 | 248,8 | 7,1 | 15,645 | 32,397 | 57,988 | 9,23806 | 1,26 | Nd |
| 7 | 09:03:26 | 09.08.2021 | 249,7 | 7,3 | 15,415 | 32,573 | 57,988 | 9,23806 | 1,26 | Nd |